

Methane flux determination in an urban wetland via Eddy Covariance

Kalimna Marion Roe-Simons

November 2019

Thesis submitted in accordance with the requirements of the University of
Adelaide for an Honours Degree in Environmental Geology



THE UNIVERSITY
of ADELAIDE

METHANE FLUX DETERMINATION IN URBAN WETLAND VIA EDDY COVARIANCE.

RUNNING TITLE:

Methane flux quantification in urban wetlands.

ABSTRACT

Methane (CH₄) is the second most potent greenhouse gas in the atmosphere after carbon dioxide. Demand for more urban green spaces, such as wetlands, as a way to combat climate change and improve biodiversity is increasing. However, there is limited literature on the impacts of climate change on these artificial systems as well as the potential contribution that these wetlands might make to climate change. Wetlands as a greenhouse gas source or sink are poorly defined due to the wide variety of wetland ecosystem and the challenges involved in long term monitoring of these gases. New robust technology for measuring methane concentration over long durations is now available in the form of eddy covariance flux towers. This study aims to apply this technique to an urban wetland in Adelaide, South Australia, thereby adding to knowledge of the urban carbon budget. Methane fluxes in the artificially constructed Urrbrae Wetlands were measured continually over three months using an eddy covariance flux tower. Mean methane flux (FCH₄) of the wetland was found to be $0.2603 \pm 0.1865 \mu\text{mol m}^{-2} \text{s}^{-1}$ which is a factor of 10 higher than typical values found in previous studies for natural wetlands. There is no statistically significant difference between mean night and daytime FCH₄. Linear correlations between FCH₄ and air temperature, air pressure and wind speed were observed. A peak in the early afternoon occurred diurnally, which coincided with the mean maximum daily temperature. No longer-term patterns were observed for the duration of the study. It is concluded that artificial urban wetlands are potentially a significant source of atmospheric methane which requires further investigation.

KEYWORDS

Methane, greenhouse gas, Eddie Covariance, wetlands, Australia, Flux.

TABLE OF CONTENTS

Running title	i
Abstract.....	i
Keywords.....	i
List of Figures and Tables	iii
1 Introduction	1
2 Theory	5
3 Site Description.....	9
4 Methods.....	12
4.1 Eddy covariance measurements.....	12
4.2 Data Processing	13
4.3 Carbon isotopes in the Urrbrae Wetland	16
5 Observations and Results	17
5.1 Overall CH ₄ fluxes.....	17
5.3 Flux Footprint.....	19
5.2 Directional Analysis	21
5.4 Diurnal Patterns	24
5.5 Monthly Variability	25
5.6 Regression analysis between methane flux and other variables.....	26
5.7 Carbon isotope ratios in wetland methane.....	27
6 Discussion	28
6.1 Quantification of methane flux.....	28
6.3 Diurnal patterns:	32
6.4 Longer-term patterns:	33
6.2 The impact of climatic factors on wetland methane flux	33
6.5 Carbon isotope ratios in wetland methane.....	35
6.6 Implications	36
6.7 Future research	37
7 Conclusions	38
8 Acknowledgments.....	39
9 References	39
Appendix A: Supplementary methods.....	43
Appendix B: Site distribution and infrastructure.....	45
Appendix C: Alternate methodology for sediment and air gas collection and analysis.	46
Appendix D: Examination of outlier values	48
Appendix E: Two sample T-tests assuming unequal variance	50

Appendix F: Sample of attempted gap-filling techniques 52

LIST OF FIGURES AND TABLES

Figure 1: (a) Location of Adelaide, with respect to South Australia and Australia. (b) Urrbrae Wetlands with respect to Adelaide Central Business District (CBD). (c) Satellite Image of Urrbrae Wetlands. Yellow line denotes the wetland boundaries. Blue lines represent the location of ephemeral ponds. Green star represents the location of the EC tower. (Full infrastructure can be found in Appendix B.) (d) EC tower with labelled components. 12

Figure 2: Segmented fetch of the study site. This image also notates the estimated flux footprint at 10, 30, 50, 70 and 90% contribution intervals. The maximum theoretical fetch of the EC instrumentation is denoted in yellow. 18

Figure 3: Standard box and whisker comparison of the wetland FCH₄ data combined and separated into night and day fluxes based on sensor code. Red crosses represent outliers. N is the number of data points assessed in each category. 20

Figure 4: Wind rose directional analysis of (a) wind speed, (b) air temperature, and (c) methane flux (FCH₄) from June to August 2019. This demonstrates how wind speed/air temperature/FCH₄ and direction of wind approach are distributed at a specific location based on bearings. The size of each wedge represents the % of data from that direction of wind approach. The colour shows the proportion of data which lies in a value range (specified to the left of each plot). Figure 4a is a traditional wind rose, while Figure 4b and 4c superimpose air temperature and FCH₄ in place of the wind speed variable. 22

Figure 5: Hourly binned FCH₄ data from study period compared with the average daily temperature trend for hourly averaged temperature data (no data gap-filling used). The number of data points used for each bin varied from 9 to 32 in each hour, with the minimum occurring at the 17th hour and max at the 10th hour. Constructed by placing half hourly intervals into hourly bins by the recorded timestamp and plotted by hour of day. I.e. Hour 1 = 00:00 to 01:00. 24

Figure 6: Average daily flux from July 7th to August 31st over the Urrbrae Wetlands. (*note there are days where no data was collected). Red crosses represent outliers from each day's distribution, individual red lines represent days where only one data point is present. 25

Figure 7: Regression analysis of various external factors with methane flux. Each factor is plotted against methane flux, then examined using least squares regression, and Pearsons correlation coefficient. (a) Compares FCH₄ with wind speed; (b) compares FCH₄ with air temperature; (c) compared FCH₄ with air pressure. 26

Figure 8: The relationship between decreasing roughness length with methane flux indicates a threshold value where the FCH₄ decrease outside the levels of instrument sensitivity. 44

Figure 9: Full infrastructure map of the Urrbrae Wetlands. 45

Figure 10: Schematic of the gas collection instrument designed by Dr Murray Hamilton used to collect air samples from near the Li7700 methane analyser. 46

Figure 11: Schematic of the instrument used for the volume displacement method. 46

Figure 12: Figure 5 (Hourly diurnal fluxes plotted with hourly average temperature) with outlier reference codes. 48

Figure 13: Copy of figure 6 (Daily flux distribution) with outlier codes. 49

Figure 14: Comparison of air temperature with methane flux using spline. Crosses represent the original data sets. 52

Table 1 Average flux footprint estimates from filtered data as distance from the EC tower in metres. N is the number of successfully recorded footprint values for each dataset. 19

Table 2: Summary of mean FCH₄ ($\mu\text{mol m}^{-2} \text{s}^{-1}$) values in Urrbrae Wetlands for the period June to August 2019. N= number of data points for the combined data set. Full statistical results are located in Appendix E. 20

Table 3: Isotopic analysis of $\delta^{13}\text{C-CH}_4$ emitted from the Urrbrae Wetland lake sediment and surrounding atmosphere. Sediment samples were tested twice each and recorded as tests (a) and (b). 27

Table 4: Literature methane flux values as reported and converted to comparable units. Where deviations were reported in the source article, they have been recorded here. 28

Table 5: Mean FCH₄ and error in the mean associated with varying roughness length. 43

Table 6: Sample of Figure 5 outliers and selected data on each interval. 48

Table 7: Sample of Figure 6 outliers with selected conditional data for each interval.49
Table 8: Comparison of Day/Night data for each data set using Two-sample t-test assuming unequal
variances. This was performed for all data combined, the wetland sector, the cattle sector and the urban
sector.50
Table 9: Comparison of Morning/Afternoon data for the wetland dataset using Two-sample t-test
assuming unequal variances.51

1 INTRODUCTION

Methane (CH₄) is the second most impactful greenhouse gas (GHG) in the atmosphere after carbon dioxide (IPCC, 2014a). This colourless, odourless gas has 84 times the global warming potential (GWP) of carbon dioxide (CO₂) over decadal timescales, and 28 times the GWP over centennial timescales (IPCC, 2014a). Methane is strongly associated with positive climate feedbacks, as observed in long term atmospheric data (Isaksen et al., 2014; Whiting & Chanton, 2001). Since the industrial revolution, methane accounts for approximately 20% of the Earth's warming, with atmospheric concentrations increasing by 150% since 1750, compared to a 40% increase in CO₂ over the same period (IPCC, 2014a; Kirschke et al., 2013).

Next to fugitive coal seam gas, landfills and agriculture, wetlands are among the largest of the world's methane emitters (Hatch, Kennedy, Hamilton, & Vincent, 2018; Shao, Sheng, Wu, Wu, & Ning, 2017). Wetlands have hydric sediments that often experience permanent anoxia, particularly in locations of high organic carbon burial, with the dominant vegetation being hydrophytic species, i.e. species which grow fully or partially in water (Blackwell, 2011). Methane is produced in anoxic wetland sediments via the process of methanogenesis, whereby bacteria decompose organic matter (OM) through sequential chemical reductions of the OM and other present elements (Blackwell, 2011; Clark, 2014; Yao & Conrad, 2000; Yvon-Durocher et al., 2014). The methane gas is then transported out of the sediment and into the atmosphere through the mechanisms of diffusion, ebullition (bubbling) and plant-mediated transportation (Blackwell, 2011; Zhu et al., 2017). Factors effecting ebullition rates include wind, air pressure and

physical disruption (i.e. from wildlife), among others (Poindexter & Variano, 2013; Tokida et al., 2007).

Urban growth has been responsible for the destruction of natural wetlands globally; now many cities are creating artificial wetlands as conduits for excess surface water, such as stormwater (Grant, Levin, Mehring, Cook, & Evrard, 2017; IPCC, 2014). While methane sourced from natural and reconstructed wetlands is usually categorised as a biogenic source, methane sourced from artificially constructed wetlands are considered as an anthropogenic source. These urban wetlands are largely unquantified as methane sources or sinks. Consequently, for cities to address climate change, planners and decision makers must be well equipped with evidence to develop climate mitigation strategies and plan sustainable and beneficial green spaces; this study is designed to add to that evidence.

Predicting the overall contribution of a given wetland system to climate change is problematic due to opposing direct effects and complex feedback processes (Blackwell, 2011). Whether a wetland is a net carbon source or sink is greatly dependent on the rate of carbon sequestration versus the rate of methane emission (Kirschke et al., 2013; Whiting et al., 2001). If CO₂ sequestration equals CH₄ output in GHG equivalents then a net neutrality of the system is achieved (Mitsch et al., 2013; Whiting et al., 2001). Mitsch et al. (2013) demonstrated via dynamic modelling of carbon flux that most wetlands, especially tropical and temperate wetlands, are significant methane emitters. Interestingly, the study by Mitsch et al. (2013) collated data from 14 different wetland studies and concluded over timescales on the order of 300 years, the positive effects of

carbon burial by natural wetlands is likely to outweigh the negative atmospheric impacts of methane emissions.

Methanogenic processes are known to be climatically sensitive and studies have demonstrated that the concentration of methane and the ratio of CH₄ : CO₂ emitted by terrestrial wetland ecosystems increases significantly with increasing temperature (Blackwell, 2011; Yvon-Durocher et al., 2014). Carbon sequestration rate also decreases as the system temperature increases (Blackwell, 2011; Whiting et al., 2001). The implication in the presently warming climate is therefore that the rate of methane emissions is likely to outweigh the sequestration ability of a given wetland system (Blackwell, 2011; Whiting et al., 2001). This effect is likely to be amplified in urban wetlands which intercept large quantities of carbon detritus, especially leaf litter, in addition to heavy metals. These systems can also be highly productive due to nutrient pollution (Blackwell, 2011). Essentially, urban wetlands behave as large carbon processing units which are largely overlooked during efforts to quantify urban carbon budgets. Therefore, understanding the dominant controls on methane flux from urban wetlands is increasingly significant when considering future climatic changes.

Despite methane's status as the second most impactful GHG, only a handful of long-term flux studies have been undertaken to examine the long-term controlling factors of methanogenic output in different wetland systems (see for example: Morin et al., 2014; Negandhi et al., 2019; Pawlak, Fortuniak, Siedlecki, & Zieliński, 2016; Silvey, Jarecke, Hopfensperger, Loecke, & Burgin, 2019; Yvon-Durocher et al., 2014). The broad assortment and scale of prospective methane sources, both from anthropogenic and

biogenic sources, makes it imperative that research into the methane budget is expanded (Pawlak et al., 2016).

Several methods have been applied to determine methane flux from terrestrial systems, of which Eddy Covariance (EC) is more widely used. EC involves a series of optical monitoring devices and weather instrumentation operating concurrently to measure the gas concentration transported by the vertical component of 3-dimensional wind eddies (Burba, 2005). This information is used to calculate turbulent fluxes within the atmospheric boundary layers across the area of interest (Burba, 2005). Despite the logistic and methodological complexity, EC enables estimation of the direction and exchange intensity of methane emissions averaged over large areas (Aubinet, Vesala, & Papale, 2012; Pawlak et al., 2016). Methods like EC have advantages over others, such as static or floating chamber techniques (Baldocchi, 2003), as the measurements are continuous, at a high temporal resolution, and fluxes are measured without surface disturbance (Baldocchi, 2003; Burba, 2013). Urban EC data measurements are difficult due to the number of potential sources and heterogeneity of the landscape, leading to a gap in published materials.

To our knowledge, methane sourced from constructed urban wetlands in Australia has never been quantified. The limited existing literature in Australia emphasises methane emissions from other anthropogenic sources (e.g. gas infrastructure) and coastal wetlands (Hatch et al., 2018; Negandhi et al., 2019; Whiting et al., 2001). Worldwide, recent research has focused on natural and reconstructed wetland systems, specifically from tropical and coastal regions, and northern hemisphere peat bogs (Herbst, Friborg,

Ringgaard, & Soegaard, 2011; Morin et al., 2014; Negandhi et al., 2019; Pawlak et al., 2016; Tang et al., 2018). Other studies have attempted to estimate CH₄ production from extremely artificial systems such as coal mines, rice paddies and landfills (Alberto et al., 2014; Feitz et al., 2018; Ge et al., 2018; Hatch et al., 2018; Lohila et al., 2007; Xu, Lin, Amen, Welding, & McDermitt, 2014). There is very little information available on artificial urban wetlands and the impacts of urbanisation on the carbon cycling in these systems with respect to methane flux (Morin et al., 2017). Those studies which have investigated wetland methane emissions have identified temporal patterns associated with natural methane flux; for example, greater production in summer months and during daytime intervals (Morin et al., 2014; Pawlak et al., 2016).

In this thesis, the rate of methane flux in the artificially constructed urban wetlands of Urrbrae, South Australia is quantified. The effects of different environmental factors on the rate of methane flux in this system are examined using micrometeorological measurements gathered over three months to develop a preliminary understanding of the role of an urban artificial wetland as a methane source. The primary hypothesis of this study is that the Urrbrae Wetlands are likely to be a CH₄ emitter, producing methane on the same scale as a natural wetland. Furthermore, it is hypothesised that there is a correlation between climatic factors, such as pressure, temperature and wind speed, with methane flux (FCH₄), and that fluxes vary over both diurnal and monthly cycles.

2 THEORY

Air movement near the Earth's surface (wind) can be described as a linear combination of small vertically oriented eddies which move in various directions and are

approximated by the wind direction and speed (Burba, 2005). These eddies act to sample the ground systems they interact with (Burba, 2005). These eddies pick-up/sample gas particles as they are transported from other locations. The variability of the size of eddies (mm to km) allows for different scales of information (wavelengths) to be collected. By examining the vertical component of these eddies movements, a relationship between the mixing of substances emanating from the surface (such as gas) and gases transported from other locations in the atmosphere can be defined.

In general terms, covariance is defined as the mean value of the product of the deviations of two variables from their respective means (Burba, 2005). Vertical flux of eddies can be recorded as the covariance of the vertical flux component and the concentration of the gas of interest. Eddy covariance is therefore used for the quantification of surface-atmosphere interactions, allowing for the direct determination of flux by measuring the properties of atmospheric eddies as they pass through a static sampling station taking instantaneous measurements (Burba, 2005; Moncrieff, Valentini, Greco, Guenther, & Ciccioli, 1997). The net gas flux is calculated for each half-hour interval from high frequency measurements of the vertical wind component and the gas concentration.

As eddy wavelengths range from millimetres to kilometres, the sampling rate of the various instrument needs to be high in order to record smaller eddies. The sampling instruments record gas concentrations and weather conditions simultaneously at 10 Hz. As atmospheric eddies, or turbulent flows, tend to be chaotic and unpredictable, it becomes necessary to collect large sets of data to get viable estimates of flux. Statistics

are calculated so the data may be filtered to allow only data of interest to be examined (Burba, 2005; Moncrieff et al., 1997). These statistics include the residual signal strength indicator (RSSI) which estimates the quality of the optical path on the methane sensor giving a value between 0-100 (e.g. excess rain and fog reduce RSSI). The program also provides quality control flags for all gas fluxes, and for a series of other factors, based on methods developed by Göckede, Markkanen, Hasager, and Foken (2006) and Mauder and Foken (2004).

Eddies are sampled to determine a net difference in concentration of the gas moving across the surface (Burba, 2005). When the vertical wind component of a given eddy is negative (i.e. flowing down), the eddy is carrying gas from outside the area sampled by that eddy. When the vertical wind component is positive (flowing up), it is assumed that the eddy is carrying gases from outside the area sampled, but it is also picking up any gases being produced in the eddy space. The difference between the gas concentrations produced when the wind is going up and down reflects the amount of gas produced in the space sampled by the eddy. A positive flux value is indicative of net production of the gas of interest and a negative indicated sequestration at the surface. Mathematically (in its simplest form), flux is defined as the mean product of instantaneous air density (ρ_d), instantaneous vertical wind speed (w) and the dry mole fraction (s), often referred to as the mixing ratio, of the gas (i.e. the concentration data collected by the instrumentation used in this study), in this case methane (Burba, 2005; Moncrieff et al., 1997):

$$F = \overline{\rho_d w s} \quad (1)$$

the overbar in Equation 1 is the time average operation; in this study, data were averaged over 30 minute intervals.

Using Reynolds decomposition, Equation 1 may be expressed as:

$$F = \overline{(\rho_d + \rho'_d)(\bar{w} + w')(\bar{s} + s')} \quad (2)$$

ρ'_d , w' and s' are the sample perturbations from the mean for each sample of data collected. Equations 1 and 2 are equivalent.

Expansion of this leaves us with:

$$F = \overline{(\rho_d \bar{w} \bar{s} + \rho_d \bar{w} s' + \rho_d w' \bar{s} + \rho_d w' s' + \rho'_d \bar{w} \bar{s} + \rho'_d \bar{w} s' + \rho'_d w' \bar{s} + \rho'_d w' s')} \quad (3)$$

This expression can be simplified. The averaged deviations of the average values are removed as they are zero. This leaves the equation:

$$F = \overline{(\rho_d \bar{w} \bar{s} + \rho_d \overline{w' s'} + \bar{w} \overline{\rho'_d s'} + \bar{s} \overline{\rho'_d w'} + \overline{\rho'_d w' s'})} \quad (4)$$

If we assume air density fluctuations are negligible, Equation 4 is further simplified to:

$$F = \overline{(\rho_d \bar{w} \bar{s} + \rho_d \overline{w' s'})} \quad (5)$$

Finally, if the mean vertical flow is also assumed negligible then flux is dependent on only the mean air density and the mean covariance between instantaneous vertical wind speed deviations and mixing ratio (Burba, 2005):

$$F \approx \overline{\rho_d \overline{w' s'}} \quad (6)$$

This assumption of negligible air density variation with elevation holds in all reasonably homogenous/flat terrains, and is generally used all conditions except mountainous regions (Burba, 2005). The assumption of little air density variation with elevation can, on occasion, be broken on sloping sites, however this does not apply to wetlands.

Further explanations of the eddy flux method are found in Baldocchi (2003), Burba, (2005) and Massman (2000).

As measurement conditions are never perfect there are many additional corrections included in data processing. These corrections account for a wide range of frequency response corrections, as well as spectroscopic and Webb-Pearman-Leuning (WPL) corrections. Frequency corrections relate to differences in the response time for the instruments used to measure concentration and meteorological variation. Frequency corrections also correct for variations in instrument response in both path and volume averaging, sensor separation, low and high pass filtering, and digital sampling. Spectroscopic error corrections compensate for variations in direct laser response between the methane and carbon dioxide sensors, while the WPL correction accounts for the changes in gas density with temperature variation (Burba, 2005; Moncrieff et al., 1997; Webb, Pearman, & Leuning, 1980).

While a large quantity of data is collected for a flux study, it is common for 80% of the data to be filtered out using these previously described statistics, and not used as much of the data are not collected under ideal eddy covariance conditions. For example, these statistics, such as RSSI determine the quantity of remaining data by indicating the quality of each interval of data.

3 SITE DESCRIPTION

The study site for this project was located at the Urrbrae Wetlands, in Adelaide, South Australia (Figure 1). Opened in 1997, the Urrbrae Wetlands are artificially constructed wetlands with a clay lining. The site spans approximately 6 ha, with a catchment area of 380 ha (Mitcham City Council, 2019). Designed to function as a water retention basin with characteristics of a natural wetland (Mitcham City Council, 2019), Urrbrae Wetlands catch 360 million litres annually, while playing host to a diversity of plant and

animal species (Mitcham City Council, 2019). The wetlands have two stormwater inlets, two sedimentation basins and one retention basin which together stores up to 17.7 million litres of water. The main pond is fitted with infrastructure which maintains a constant water level by controlling in-flow and out-flow rates. The wetland uses sedimentation, filtering, nutrient up-take by plants, organic oxidation, and UV sterilisation to prevent further transportation of incoming stormwater pollutants.

The landscape surrounding the Urrbrae Wetlands has been revegetated with a variety of native species with the aim of restoring the vegetation to a state similar to that seen prior to European settlement in 1836. The edge of the aquatic zone is dominated by the common reed (*Phragmites australis*), and two species of sedge. Extending further from the water's edge occurs a mixture of vegetation with an upper storey mostly comprising of various *Eucalyptus* species, and an under storey dominated by *Acacia*. The ground cover is primarily native grasses and saltbush. Previous scientific work in the Urrbrae Wetlands has been limited, bar a study to test filtering methodologies to improve water quality (Dillon, Pavelic, Massmann, Barry, & Correll, 2001).

There is a cattle paddock approximately 80 m south of the sampling site; it is well known that cattle are major sources of methane (IPCC, 1990). The area to the west of the site is mostly suburban housing. There may be additional sources of methane originating from this area as well, possibly related to gas infrastructure and other sources related to urban settings (Hatch et al., 2018). A major east-west arterial road runs immediately north of the study site; this is the major channel for incoming water from surrounding roads and suburbs. As we are interested in gas sourced from the

wetland, data collected from this direction will be separated out and processed individually from the main sampling area.

Data for this study were collected from June to August 2019, i.e. southern hemisphere winter. The climate in Adelaide is a generally mild, Mediterranean, temperate climate. The winter months are characterised by mild daytime temperature, cool evenings, and intermittent rain. The recorded total monthly rainfall for the region was 32.2, 47.1 and 58.4 mm from the months June to August (Bureau of Meteorology, 2019). Australian Bureau of Meteorology data indicates that the average maximum monthly temperatures for 2019 were 16.3, 16.4, and 15.6⁰C for the months of June, July and August respectively, and monthly minimum values of 7.5, 8.9, and 7.3⁰C respectively (Bureau of Meteorology, 2019). Shading from surrounding vegetation results in obscured early and late day sunlight hours on the wetland, hence direct sunlight exposure occurs only during the late morning to mid-afternoon.

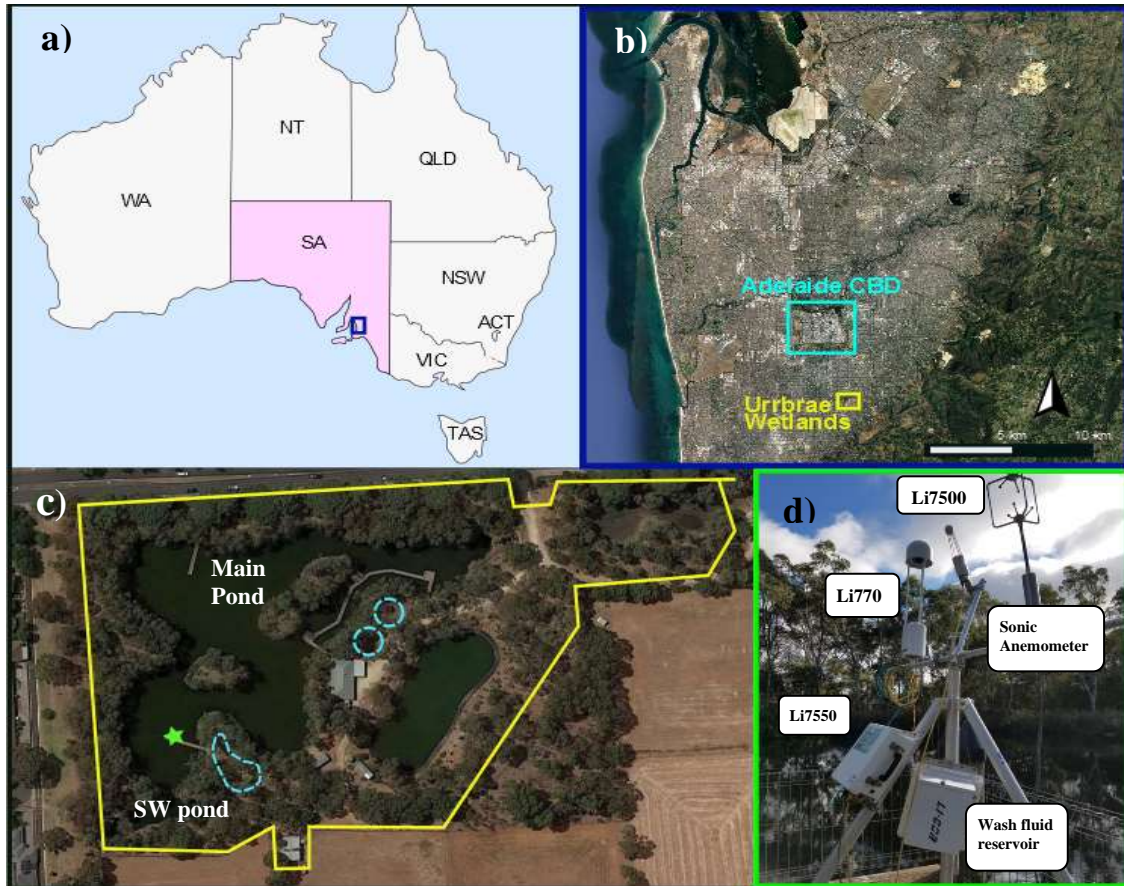


Figure 1: (a) Location of Adelaide, with respect to South Australia and Australia. (b) Urrbrae Wetlands with respect to Adelaide Central Business District (CBD). (c) Satellite Image of Urrbrae Wetlands. Yellow line denotes the wetland boundaries. Blue lines represent the location of ephemeral ponds. Green star represents the location of the EC tower. (Full infrastructure can be found in Appendix B.) (d) EC tower with labelled components.

4 METHODS

4.1 EDDY COVARIANCE MEASUREMENTS

The equipment is depicted in Figure 1d and is set up to collect as much data as possible from the main pond (Figure 1c). As such, the sampling site is located over the main pond at the end of the south-west jetty ($34^{\circ}57'57.956''\text{S}$, $138^{\circ}37'4.786''\text{E}$, 300 m a.s.l.). The turbulent flux of methane emitted from the Urrbrae Wetland was measured using an array of optical gas analysers attached to a small (2.93 m tall) tower located on a wooden jetty which protruded ~ 15 m into the wetland (Figure 1c and 1d).

Atmospheric methane concentrations were measured using a LI-COR LI-7700 open path methane analyser. To accurately measure methane flux, both latent and sensible heat flux were measured using an open path LI-7500 infrared CO₂/H₂O analyser. As the measurement of both vertical and horizontal wind motion is crucial to the eddy covariance method, a Gill Windmaster Pro 3-D sonic anemometer was used to record all three components of wind velocity and also “sonic temperature” (i.e. dry air temperature based on air conditions as measured in the anemometer path). The sensors were installed on the tower via horizontal arms orientated east-west (Figure 1d), with the sonic anemometer installed on the eastern side of the arm, and the CO₂/H₂O sensor on a raised arm over the centre mast so the centre of its sensor path aligned with the sonic anemometer. Finally, the methane sensor was situated 42 cm west of the anemometer. The centre of the methane analyser’s path sat 19 cm below that of the sonic anemometer due to structural limitations (Figure 1d). The sensors recorded air temperature, wind speed, and CO₂ and CH₄ fluctuations at a sampling rate of 10 Hz. (10 samples per second) with a precision < 5 ppb. The data from these sensors were then collated in the LI-7550 smart flux data logger. The LI-7550 interface was mounted on the south-west leg of the tripod base to avoid impacting the measurements. As concentration data were dependant on both inbuilt mirrors and lasers, it was necessary to keep these clean both manually and through use of an automatic cleaning system. The LI-7550 was also equipped with a secondary ambient temperature probe, and an air pressure sensor.

4.2 DATA PROCESSING

All the data collected for this study were processed using LI-COR’s EddyPro[®]7 open-source software (LICOR, 2019). This program creates 30-minute averaged files of highly sampled raw data; calculating the required covariances (see Theory section), as

well as the correction factors needed to calculate the fluxes. The final EddyPro output contains 187 different variables (both calculated and raw) averaged for each 30-minute interval for the entire collection period. Most of these variables are statistics and data quality estimates that allow quality control over the various measured fluxes.

Data were filtered based on the statistics provided by EddyPro. A specific set of environmental conditions are required to make robust estimates of gas flux using EC, such that a proportion of the collected data needs to be filtered out due to failure to meet key criteria. For example, one factor affecting the data quality is excessive rain or fog which interferes with the sample path on the concentration instrumentation (LI-7700 and LI-7500). Data under these conditions need to be filtered out. As previously described, another factor examined was RSSI; for this study, intervals demonstrating $RSSI \geq 40$ were deemed acceptable.

As part of the data processing output from EddyPro, estimates of flux footprint are provided. The flux footprint is an estimate of the location and relative contributions of sources influencing flux measurements at a given sensor height, depending on height, atmospheric stability, and surface roughness (Burba, 2005; Kljun, Calanca, Rotach, & Schmid, 2004). The flux footprint data provides information on the source area defined as a set of distances. The 10%, 30%, 50%, 70%, and 90% footprint distances, are the area between the anemometer and the distance which provides the respective percentage of the total flux. The peak distance is the distance which makes the individual largest contribution of flux of data for each recorded interval. The average peak distance is the mean distance which contributes fluxes of largest magnitudes. For example, given a

value of 50 m for a 90% statistic, this means 90 % of the data originates within a 50 m radius of the EC tower. These estimates are calculated by EddyPro following the method of Kljun et al. (2004).

Over three months of monitoring, 4261 measurements of a potential 4416 were successfully recorded. Of these successful intervals, 1042 data points (24%) were retained after quality control filters were applied. Holes exist in the data due to a number of issues. These include problems maintaining power during some of the extended periods of rainfall and low sunlight conditions that occurred during the study (for example, from August 7th to 13th). This caused intermittent failures in the power system when the solar panels received insufficient sunlight to keep the battery system fully charged. Additionally, there were initial mechanical issues with the methane sensor which resulted in excess data loss from June 12th to July 18th. At other times the weather conditions were unable to collect sufficient information for flux estimations; such as 1st to 3rd August.

A final filtering step to isolate flux data derived from the wetland specifically, rather than potential other sources surrounding the wetland, was applied. This was achieved by filtering data according to wind direction. Since the tower was located at the south-east margin of the wetland, only data collected during wind flow originating from -22.5 to 90° was retained as wetland data (Figure 2).

All secondary data processing to construct figures was performed in MATLAB (V. 2018b) and Excel. These processes include filtering for angle of wind approach, sorting

data by different factors (date, time, angle of approach, etc.) for the identification of patterns, and the assessment of the impact of various environmental factors. Further details on methodology can be found in Appendix A.

4.3 CARBON ISOTOPES IN THE URRBRAE WETLAND

Air samples were collected from the same vicinity as those collected by the LI-7700 using gas collection bags placed inside a plastic box, attached to an intake valve (Hamilton, 2019, unpublished) (Full methodology available in Appendix C).

Samples of sediment gas were collected using a column displacement method. A funnel (diameter 30 cm) was attached to a clean, dry 250 mL water bottle, with a handle supporting for ease of use. The equipment was inverted underwater and the bottle allowed to fill. The sediment was disturbed manually under the area of the funnel to encourage the bubbles to rise into the bottle and displace the water. Once filled with gas, the bottle was unscrewed from the funnel and capped while still underwater, hence no gas was lost or contaminated with air. The area sampled for each bottle was approximately 2 x 4 m. These sediment samples and the air samples were returned to the laboratory and analysed for isotopic ratio using a Picarro gas analyser (Model G2201-I).

The Picarro gas analyser was first allowed to sample the room air, and then flushed with a gas standard (2.075 ppm CH₄). The air samples were tested by drawing air directly from the gas sample bags into the Picarro. The bottle sediment gas samples were first diluted by mixing 0.2 mL of sediment gas with 500mL of zero air before testing.

Between each test the Picarro was allowed to draw surrounding air. (See Appendix C for further theory, methodology, and diagrams).

5 OBSERVATIONS AND RESULTS

5.1 OVERALL CH₄ FLUXES

Flux data collected at the Urrbrae site is likely to have a number of sources. To address this, the study area has been separated into three different source-type segments characterised by wind direction. The primary segment of interest is the main wetland which lies from compass bearings 337.5 to 90⁰ relative to the location of the monitoring tower. The area to the southeast and south (90 – 220⁰) is dominated by a cattle paddock but also contains farmland and the Urrbrae High School. The final section to the west (220 – 337.5⁰) is predominantly urban environment (Figure 2). Examination of the study area shows that while the major sources in each segment have been defined, there are likely to be contributions from other sources in each area. These will be evaluated in subsequent sections of this paper. Henceforth the data collected from these regions are referred to as the wetland sector, cattle sector and urban sector respectively.



Figure 2: Segmented fetch of the study site. This image also notates the estimated flux foot footprint at 10, 30, 50, 70 and 90% contribution intervals. The maximum theoretical fetch of the EC instrumentation is denoted in yellow.

Flux footprint and FCH₄ from each of the sources defined over the entire field area are presented in Table 1 and Table 2. These data, and all data discussed from this point forward are the quality controlled, filtered data unless otherwise specified or further constrained.

5.3 FLUX FOOTPRINT

Table 1 Average flux footprint estimates from filtered data as distance from the EC tower in metres. N is the number of successfully recorded footprint values for each dataset.

Direction	Statistic	Peak distance	10%	30%	50%	70%	90%
All	Mean	52.79	18.12	45.12	68.81	96.51	144.60
N = 367	Std.dev	8.66	2.97	7.41	11.29	15.84	23.73
Wetland	Mean	48.97	16.81	41.86	63.83	89.52	134.12
N = 197	Std.dev	6.78	2.33	5.79	8.83	12.39	18.56
Cattle	Mean	63.83	21.92	54.58	83.24	116.74	174.90
N = 43	Std.dev	12.40	4.26	10.60	16.16	22.67	33.96
Urban	Mean	55.18	18.94	47.16	71.93	100.88	151.14
N = 127	Std.dev	5.35	1.84	4.58	6.99	9.79	14.66

Over all directions, the largest FCH₄ flux (peak) contributions to the entire area were estimated to have derived from a 53 m radius around the anemometer, with 90 % of the dataset collected within 145 m. This is consistent with the primary contributions originating from within the wetland (Table 1). The wetland sector refines this further where the peak fluxes originate from a 49 m radius and 90 % of the data is collected within 134 m of the anemometer (Table 1). To visualise the space with respect to the footprint values, the various contribution distances from the wetland sector can be seen in Figure 2.

Table 2: Summary of mean FCH₄ ($\mu\text{mol m}^{-2} \text{s}^{-1}$) values in Urrbrae Wetlands for the period June to August 2019. N= number of data points for the combined data set. Full statistical results are located in Appendix E.

Source	Time of Day	Average FCH ₄ ($\mu\text{mol m}^{-2} \text{s}^{-1}$)	Standard Deviation ($\mu\text{mol m}^{-2} \text{s}^{-1}$)
All Sources ¥ (0 – 360 °) N = 1043	Combined	0.2469	0.2028
	Night	0.2432	0.1994
	Day	0.2516	0.2072
Wetland * (-22.5 – 90 °) N = 422	Combined	0.2603	0.1865
	Night	0.2197	0.1391
	Day	0.3081	0.2211
Cattle Paddock * (90 – 220 °) N = 406	Combined	0.2493	0.2231
	Night	0.2773	0.2398
	Day	0.1699	0.1399
Urban * (220 – 337.5 °) N = 215	Combined	0.2162	0.1907
	Night	0.2573	0.2377
	Day	0.2103	0.1886

*T-tests comparing night and day fluxes for these data sets all gave $p < 0.05$.

¥T-tests comparing night and day fluxes for these data sets all gave $p > 0.05$.

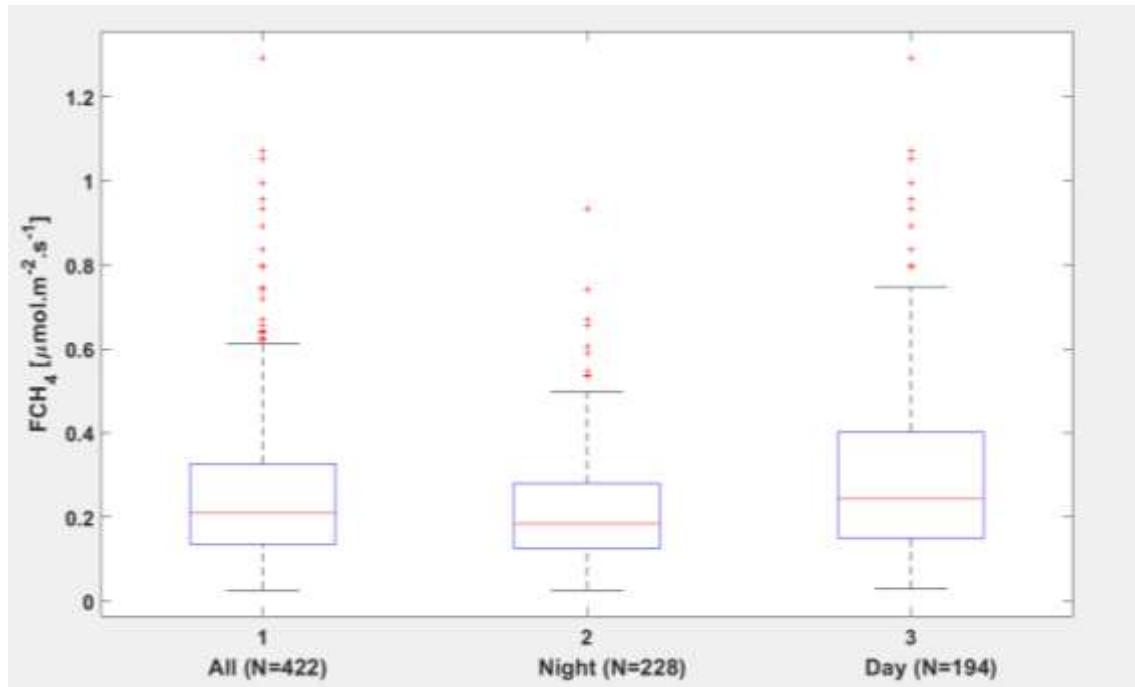


Figure 3: Standard box and whisker comparison of the wetland FCH₄ data combined and separated into night and day fluxes based on sensor code. Red crosses represent outliers. N is the number of data points assessed in each category.

Positive flux values are defined as a methane ‘source’. The overall average FCH_4 calculated in the wetland sector was $0.2603 \pm 0.1865 \mu\text{mol m}^{-2} \text{s}^{-1}$ (Table 2). Higher FCH_4 was measured during the day ($0.3081 \pm 0.2211 \mu\text{mol m}^{-2} \text{s}^{-1}$) compared to those measured at night ($0.2197 \pm 0.1391 \mu\text{mol m}^{-2} \text{s}^{-1}$) (Table 2). Many outliers from the distribution can be observed (Figure 3). The spread of data for the night and daytime distributions also heavily overlap (Figure 3). While daytime fluxes are slightly higher, they demonstrate a larger spread of data than the night fluxes, excluding outliers. There are a similar number of outliers present in both data sets, and interestingly all the outliers tend to be above the observed distributions.

The FCH_4 contributed by the cattle paddock sector were on average $0.2493 \pm 0.2231 \mu\text{mol m}^{-2} \text{s}^{-1}$ and unlike the wetland, higher fluxes were observed during the night ($0.2773 \pm 0.2398 \mu\text{mol m}^{-2} \text{s}^{-1}$) compared to the day ($0.1699 \pm 0.1399 \mu\text{mol m}^{-2} \text{s}^{-1}$) (Table 2). The FCH_4 from the urban sector were on average $0.2162 \pm 0.1907 \mu\text{mol m}^{-2} \text{s}^{-1}$ and also unlike the wetland, slightly higher fluxes were observed during the night ($0.2573 \pm 0.2377 \mu\text{mol m}^{-2} \text{s}^{-1}$) compared to the day ($0.2103 \pm 0.1886 \mu\text{mol m}^{-2} \text{s}^{-1}$) (Table 2).

5.2 DIRECTIONAL ANALYSIS

Analysis of various climatic factors based on wind approach is required to understand the spatial distribution of the methane sources and the relative contributions these sources make to the measured FCH_4 . The distributions of wind direction as compared with the relative contributions of a specific factor are plotted in Figure 4.

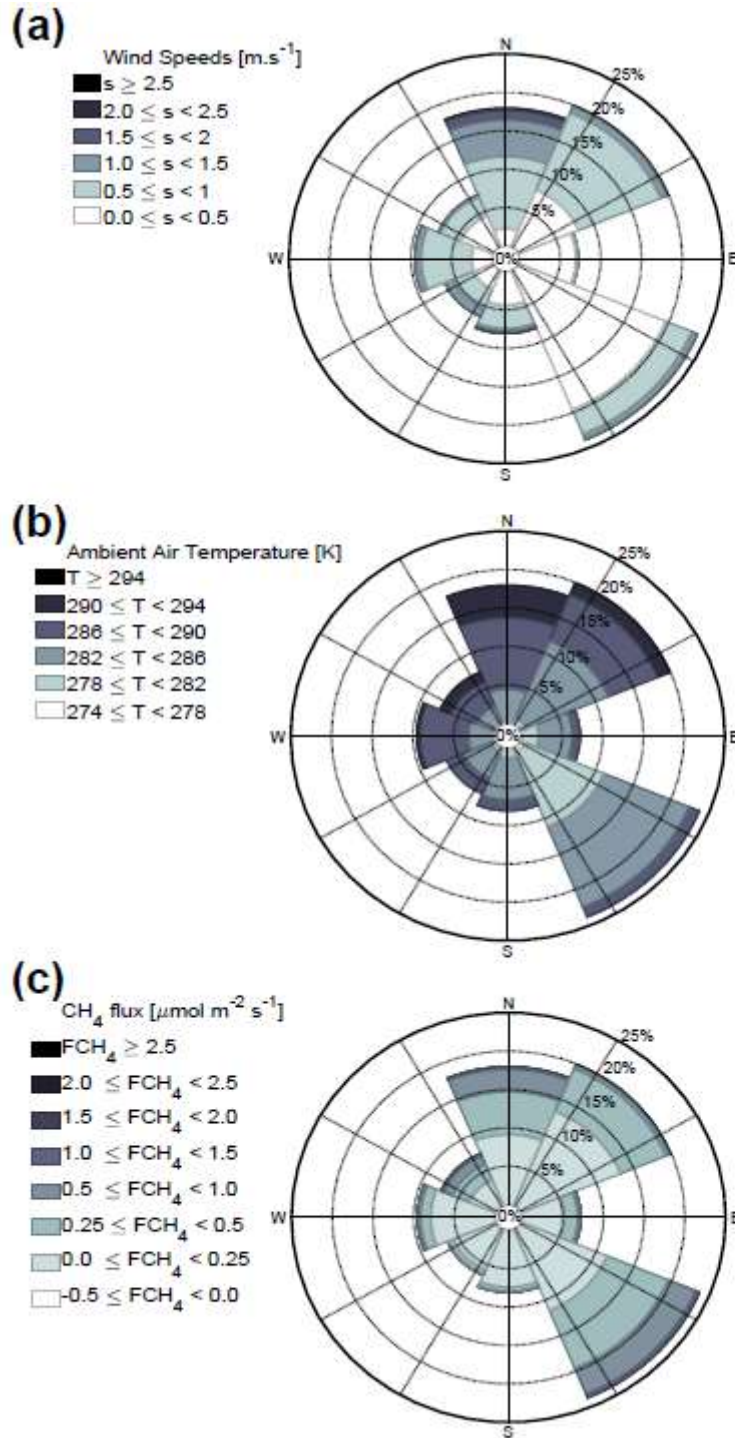


Figure 4: Wind rose directional analysis of (a) wind speed, (b) air temperature, and (c) methane flux (FCH_4) from June to August 2019. This demonstrates how wind speed/air temperature/ FCH_4 and direction of wind approach are distributed at a specific location based on bearings. The size of each wedge represents the % of data from that direction of wind approach. The colour shows the proportion of data which lies in a value range (specified to the left of each plot). Figure 4a is a traditional wind rose, while Figure 4b and 4c superimpose air temperature and FCH_4 in place of the wind speed variable.

Wind rose analysis showed the dominant wind directions originated from the north, north-east and south west over the time this survey was conducted (Figure 4a).

The main zones of data collection originate from the north and north easterly directions, from the wetland sector (49% of data), and from the south easterly winds, from the cattle paddock sector (19% of data) (Figure 4a). The northerly winds were generally the highest velocity with wind speeds $> 2.5 \text{ m.s}^{-1}$ (9 km.h^{-1}) approximately 0.5 % of the time. In the wetland sector, a mean wind speed of 0.7 m.s^{-1} was recorded compared to 0.6 m.s^{-1} across the entire study site. The majority of the winds across the study region were less than 0.5 m.s^{-1} (1.8 km.h^{-1}) from all directions. These wind speeds are likely limited as a result of the shelter from topography and vegetation covering the site.

The warmest temperatures from June to August occurred during periods of wind originating from the north-west, north, and north-east. It is likely this is an effect of the topography and vegetation located onsite limiting sun exposure (Figure 4b). The average measured air temperature for the three months was 12.4 , 12.0 and $12.2 \text{ }^{\circ}\text{C}$ for June, July and August respectively, as calculated from successful sampling days only with sample sizes of 7, 16 and 27 days respectively.

FCH_4 levels were highest over the wetlands sector and cattle sector (Figure 4c).

Significant FCH_4 contributions were also measured from the urban sector (Figure 4c).

5.4 DIURNAL PATTERNS

To examine the role of diurnal cycles in methane flux, FCH_4 originating from the wetland sector was binned for each hour of the day and is represented in the form of a series of box and whisker plots (Figure 5). These data are compared to hourly average air temperature for the corresponding period (Figure 5).

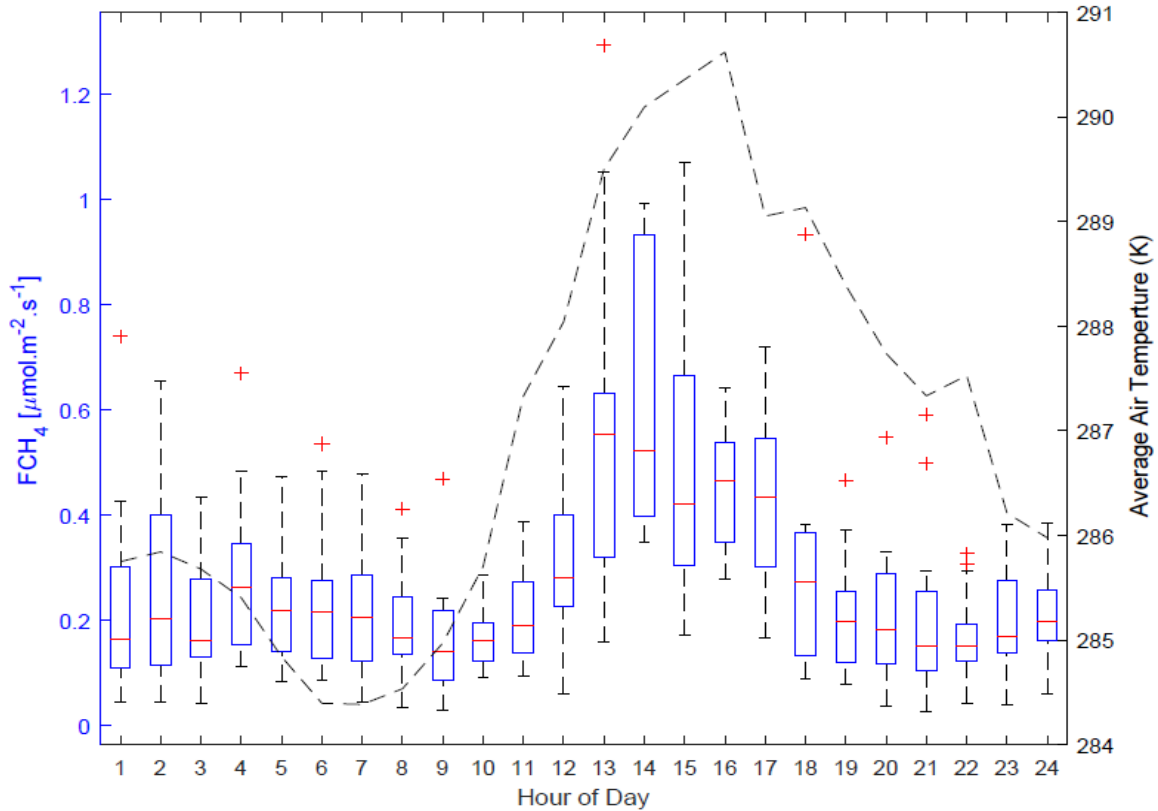


Figure 5: Hourly binned FCH_4 data from study period compared with the average daily temperature trend for hourly averaged temperature data (no data gap-filling used). The number of data points used for each bin varied from 9 to 32 in each hour, with the minimum occurring at the 17th hour and max at the 10th hour. Constructed by placing half hourly intervals into hourly bins by the recorded timestamp and plotted by hour of day. I.e. Hour 1 = 00:00 to 01:00.

The average distributions of FCH_4 levels across hourly timescales peak in the early afternoon between 14:00 and 15:00 and are relatively constant across the rest of the day (Figure 5). These afternoon peaks also demonstrate the largest amount of variability, possibly relating to the lower number of available data-points for this period. The early afternoon peak corresponds with the average maximum daily temperature (Figure 5).

Examining the interval data from a sample of the outliers from Figure 5 shows the outliers all occur between 12 – 18 °C with similar air pressure (In Appendix D this information is expanded further).

5.5 MONTHLY VARIABILITY

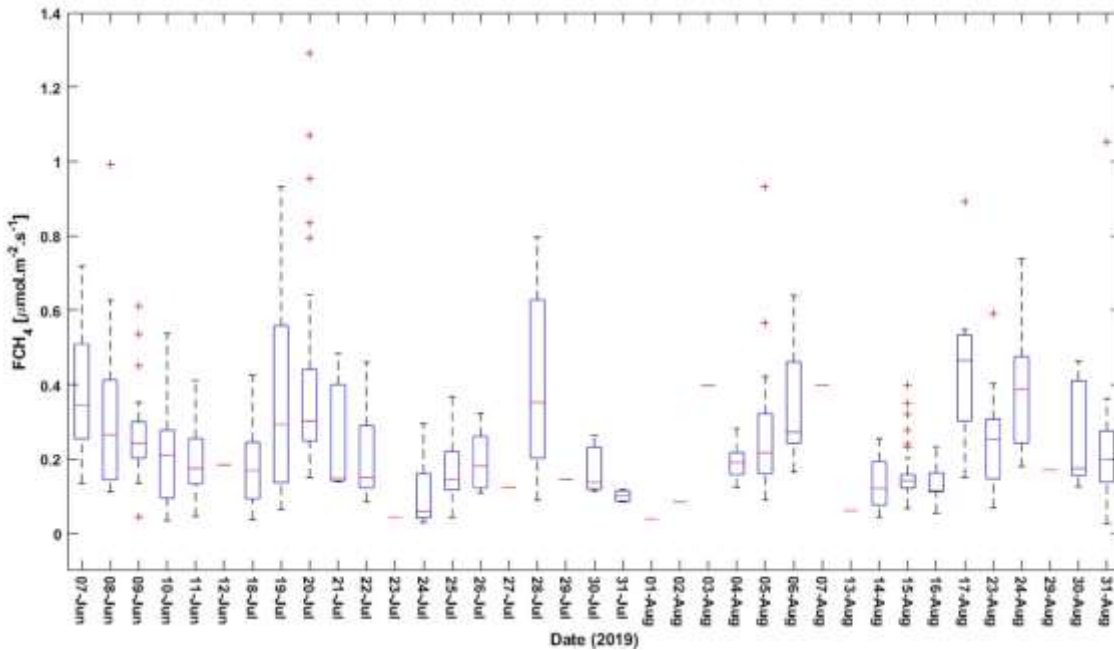


Figure 6: Average daily flux from June 7th to August 31st over the Urrbrae Wetlands. (*note there are days where no data was collected). Red crosses represent outliers from each day's distribution, individual red lines represent days where only one data point is present.

Inter-daily variability in FCH₄ is displayed in Figure 6. As the data set is not continuous it is difficult to make any strong conclusions of regarding trend, however on examination of Figure 6 it is notable that all FCH₄ from the wetland is positive, i.e. even in winter, this wetland was a net producer of methane. The highest mean daily FCH₄ (containing >1 data point) occurred on August 17th and the lowest on July 24th.

Examination of the properties of a sample of the outliers shows all outliers lie above the respective days flux distributions, and all occur during the afternoon daylight hours. (Appendix D further examines the properties of the outliers present in Figure 6).

5.6 REGRESSION ANALYSIS BETWEEN METHANE FLUX AND OTHER VARIABLES

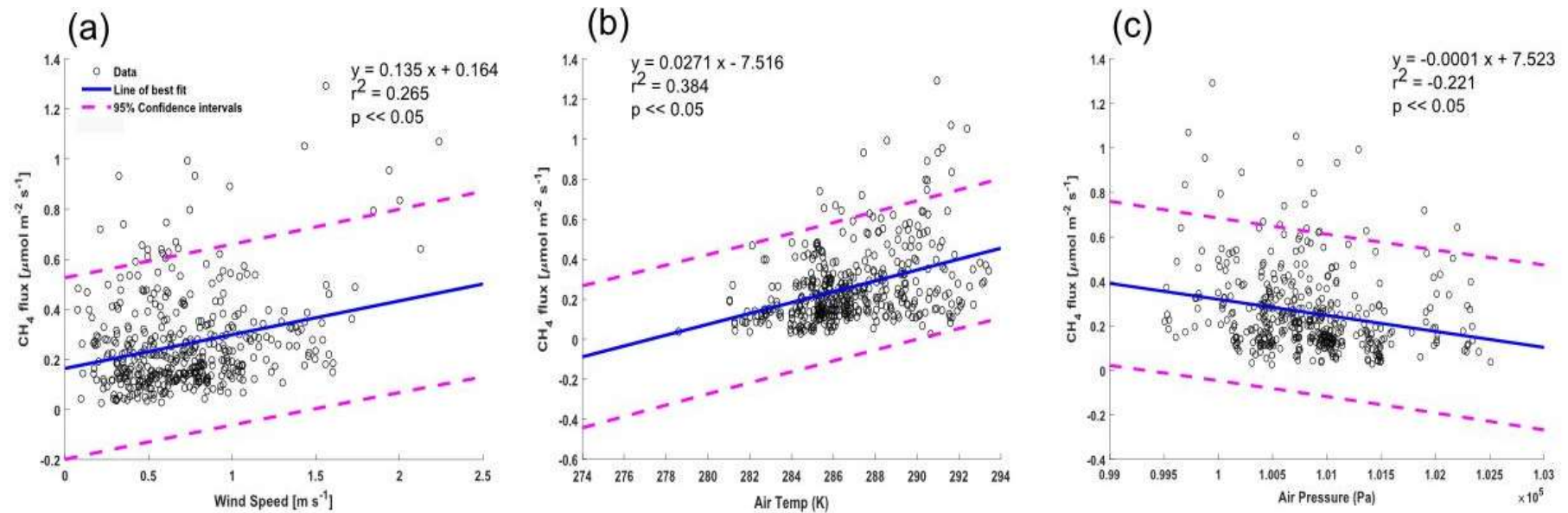


Figure 7: Regression analysis of various external factors with methane flux. Each factor is plotted against methane flux, then examined using least squares regression, and Pearson's correlation coefficient. (a) Compares FCH_4 with wind speed; (b) compares FCH_4 with air temperature; (c) compared FCH_4 with air pressure.

Statistically significant ($p < 0.05$) positive regressions were observed between FCH_4 and both wind speed ($r^2=0.265$) and air temperature ($r^2=0.384$) (Figure 7a, Figure 7b) within the wetland system. A negative regression was observed with air pressure ($r^2 = -0.221$) (Figure 7c).

5.7 CARBON ISOTOPE RATIOS IN WETLAND METHANE

Two samples of air above the wetland were found to have $\delta^{13}C-CH_4$ of -46 and -47 (Table 3). By contrast, gas sampled from the wetland sediment had $\delta^{13}C-CH_4$ of -59 (Table 3). The air samples have a higher $\delta^{13}C-CH_4$ than the sediment samples.

Table 3: Isotopic analysis of $\delta^{13}C-CH_4$ emitted from the Urrbrae Wetland lake sediment and surrounding atmosphere. Sediment samples were tested twice each and recorded as tests (a) and (b).

Source	Delta, $\delta^{13}C-CH_4$ ‰
Urrbrae Air 1	-46.5
Urrbrae Air 2	-47.9
Urrbrae Sediment 1a	-59.1
Urrbrae Sediment 1b	-58.9
Urrbrae Sediment 2a	-58.8
Urrbrae Sediment 2b	-59.1

6 DISCUSSION

6.1 QUANTIFICATION OF METHANE FLUX

Table 4: Literature methane flux values as reported and converted to comparable units. Where deviations were reported in the source article, they have been recorded here.

Paper	Reported Average CH ₄ Flux	Papers Original Units	Converted to $\mu\text{mol}/\text{m}^2/\text{s}$	Days Recorded/Period recorded	Site Description	Method Used
(Morin et al., 2014)	879.2	$\mu\text{mol} \cdot \text{m}^{-2} \cdot \text{d}^{-1}$	0.0101	98.5 days/ winter 2011-12	Temperate constructed wetland, North America	Eddy Covariance tower
(Morin et al., 2014)	1501.5	$\mu\text{mol} \cdot \text{m}^{-2} \cdot \text{d}^{-1}$	0.0174	14.1 days/ winter 2012-13		
(Morin et al., 2014)	1000	$\mu\text{mol} \cdot \text{m}^{-2} \cdot \text{d}^{-1}$	0.0116	41.8 days / summer 2011		
(Morin et al., 2014)	3205.1	$\mu\text{mol} \cdot \text{m}^{-2} \cdot \text{d}^{-1}$	0.0371	41.5 days / summer 2012		
(Tang et al., 2018)	0.024	$\text{g C-CH}_4 \cdot \text{m}^{-2} \cdot \text{d}^{-1}$	0.0174	2 months / wet season, Average all	Tropical Peat Forest Borneo	Eddy Covariance tower
(Tang et al., 2018)	29 ± 1 17 ± 0.3	$\text{nmol} \cdot \text{m}^{-2} \cdot \text{s}^{-1}$	0.029 ± 0.001 0.017 ± 0.0003	Daytime Night-time		
(Tang et al., 2018)	20.3 ± 0.8 27 ± 1 13 ± 0.6	$\text{nmol} \cdot \text{m}^{-2} \cdot \text{s}^{-1}$	0.0203 ± 0.0008 0.027 ± 0.001 0.013 ± 0.0006	November (all) Daytime Night-time		
(Tang et al., 2018)	25.3 ± 0.6 30 ± 1 20 ± 0.4	$\text{nmol} \cdot \text{m}^{-2} \cdot \text{s}^{-1}$	0.0253 ± 0.0006 0.030 ± 0.001 0.020 ± 0.0004	December (all) Daytime Night-time		
(Pawlak et al., 2016)	18.3 – 129.7	$\text{nmol} \cdot \text{m}^{-2} \cdot \text{s}^{-1}$	0.0183 – 0.1297	8 months summer (Temp eq. to our winter)	Rehabilitated peatlands in Poland	Eddy Covariance tower
(Pawlak et al., 2016)	3.2 – 81.2	$\text{nmol} \cdot \text{m}^{-2} \cdot \text{s}^{-1}$	0.0032 – 0.0812	6 months Spring (2013, 2014, 2015)		
(Pawlak et al., 2016)	11.1 – 51.6	$\text{nmol} \cdot \text{m}^{-2} \cdot \text{s}^{-1}$	0.0111 – 0.0516	7 months Autumn (2013, 2014, 2015)		
(Pawlak et al., 2016)	4.8 – 15.1	$\text{nmol} \cdot \text{m}^{-2} \cdot \text{s}^{-1}$	0.0048 – 0.0151	6 months Winter (2013, 2014, 2015)		
(Pawlak et al., 2016)	34.3	$\text{nmol} \cdot \text{m}^{-2} \cdot \text{s}^{-1}$	0.0343	Average		
(Shao et al., 2017)	1 - 23	$\text{mg} \cdot \text{m}^{-2} \cdot \text{h}^{-1}$	0.017 - 0.398	Spring	Costal Wetland, China	Transparent static chamber
(Shao et al., 2017)	5 - 38	$\text{mg} \cdot \text{m}^{-2} \cdot \text{h}^{-1}$	0.0866 - 0.658	Autumn		
(Negandhi et al., 2019)	-1.74 – -0.07 0.82 - 1.03	$\text{g C m}^{-2} \text{yr}^{-1}$ $\text{g C m}^{-2} \text{yr}^{-1}$	$-3.5 \times 10^{-3} - -1.4 \times 10^{-4}$ $1.6 \times 10^{-3} - 2.04 \times 10^{-3}$	Spring Summer/Autumn	Coastal Wetland, NSW, Australia	EC
(Deemer et al., 2016)	120	$\text{mg} \cdot \text{m}^{-2} \cdot \text{d}^{-1}$	0.0866	Average	Reservoir (Table 1 from article)	Mixture of techniques
(Melton et al., 2013)	15 - 63	$\text{mg} \cdot \text{m}^{-2} \cdot \text{d}^{-1}$	0.0108 – 0.0455	Average	Wetland	Modelling from top down datasets
(Holgerson & Raymond, 2016)	27	$\text{mg} \cdot \text{m}^{-2} \cdot \text{d}^{-1}$	0.0195	Average	Very small Ponds (SA < 0.001 km ²)	Direct measurements (unspecified)
(Herbst et al., 2011)	30.2	$\text{mg} \cdot \text{m}^{-2} \cdot \text{d}^{-1}$	0.0218	Average annual daily	Restored Wetlands, Denmark	Closed Path EC
(Herbst et al., 2011)	100 - 150	$\text{mg} \cdot \text{m}^{-2} \cdot \text{d}^{-1}$	0.0722 – 0.108	August/September (Summer – 16.8°C average)		

(Xu et al., 2014)	17.7 15.8 20.24	$\mu\text{mol} \cdot \text{m}^{-2} \cdot \text{s}^{-1}$	17.7 (all) 15.8 20.24	June – Dec 2010 June – Oct Nov - Dec	Land fill in Nebraska, USA	Open Path EC
(Lohila et al., 2007)	0.53	$\text{mg} \cdot \text{m}^{-2} \cdot \text{s}^{-1}$	33.04	June to December	Finland municipal landfill	EC
(Ge et al., 2018)	Peak value 0.20	$\mu\text{mol} \cdot \text{m}^{-2} \cdot \text{s}^{-1}$	0.20	June – November 2016	Chinese Rice field growing season	Open path EC
(Alberto et al., 2014)	0.082 ± 0.048 vegetative stage 0.063 ± 0.021 reproductive stage 0.060 ± 0.033 ripening stage	$\mu\text{mol} \cdot \text{m}^{-2} \cdot \text{s}^{-1}$	0.082 ± 0.048 vegetative stage 0.063 ± 0.021 reproductive stage 0.060 ± 0.033 ripening stage	Dec 2012 – April 2013	Philippines Rice field	Open path EC
Measured Data	0.2603	$\mu\text{mol} \cdot \text{m}^{-2} \cdot \text{s}^{-1}$	0.2603	Winter (June - August)	Urban Temperate Wetland	Open Path EC

Wetlands are a recognised global source of atmospheric methane, however few studies have been conducted on urban wetlands, which often receive uniquely high nutrient and metal pollutant loads, in addition to both autochthonous and allochthonous OM. Compared to a systematic survey of published methane emissions from global wetlands (Table 4), the measured FCH_4 from Urrbrae Wetlands is significantly higher, by a factor of 10. The Urrbrae Wetlands are the only artificially designed wetlands, which the author is aware of, with a constant water-level due to the infrastructure in place, to be examined for methane flux rates. Many of the sites studied previously are classified as natural or reconstructed wetlands, which all have unique properties of their own in terms of hydrological regulation, vegetation/peat composition, and climate (e.g. freezing during winter conditions). The flux values reported here are similar to those reported for Chinese rice fields during growing season (Table 4) (Ge et al., 2018). However, by comparison to FCH_4 from two municipal landfill sites, the measured FCH_4 emissions from Urrbrae are only ~ 1% of those (Ge et al., 2018; Lohila et al., 2007; Xu et al., 2014).

The flux footprint provides an estimate of the upwind contribution to the measured fluxes (Burba, 2005). Examination of the footprint in the wetland sector indicates that peak contributions originate within 49 ± 7 m of the EC tower, and 90% of the data is collected within a radius of 134 ± 19 m. (Table 1) This provides confidence that the primary FCH₄ origins lie within the wetland boundaries, with 70 % of the data originating from the main pond, with minimal interference from the outlying urban areas (Table 1). The cattle paddock begins 82 m from the tower and extends to 253 m from the tower. The cattle footprint peaks at 64 ± 12 m, with 90% of data originating within 175 ± 34 m, indicating that most of the cattle paddock is significant to the analysis of that sector (Table 1).

Although larger daytime FCH₄ are observed in the wetland system (Figure 3), the difference when compared to the night-time FCH₄ is not statistically significant ($p < 0.05$) (Table 2). This differs to a previous study by Morin et al. (2014) where natural wetland systems experienced higher daytime FCH₄, with small but significant night-time emissions. It would be expected that warmer wetland water temperature would result in greater FCH₄, due to the positive effect on methanogenic bacteria (Yvon-Durocher et al., 2014). However, at Urrbrae, this appears to not be a major factor, as the temperature range was small during the monitored period, and there is limited difference between day/night. This could be because the methane is trapped in the sediments, before being periodically bubbled out. This ebullition can be observed at the Urrbrae Wetlands in all weather conditions at significant rates. By testing the morning data (06:00 – 12:00) against the afternoon data (12:00 – 16:30) in the same way as the night/day comparisons, there was no statistically significant difference ($p < 0.5$)

between morning and afternoon FCH_4 (Appendix E). Periods of large ebullitive contribution may be indicated by the presence of numerous, large, positive outliers in the wetland distribution.

Similarly, this may be affecting the results obtained over the cattle sector. The FCH_4 rates observed over the cattle sector are lower during the daytime than at night, however experience greater variability causing overlap of the distributions. Statistically, the difference between day and night mean fluxes in the cattle sector, based on the students t-test were insignificant ($p < 0.05$) (Table 2). The night fluxes over the cattle dataset had greater variability in the data set. These values may reflect the presence of the sedimentation basin and ephemeral ponds which may have influenced results by skewing the flux rates.

Cattle are a second major producer of atmospheric methane present in the study area. Therefore, the FCH_4 values for the wetland sector were compared with the cattle sector. The cattle paddock usually houses 6 to 10 cattle at a time. McGinn et al. (2014) claims grass-fed cattle produce $\sim 189 \pm 6 \text{ g animal}^{-1} \text{ d}^{-1}$ of methane, that is approximately $136 \pm 4 \text{ } \mu\text{mol animal}^{-1} \text{ s}^{-1}$ (McGinn et al., 2014). Assuming there are 8 animals (on average in cattle paddock) and the area of the paddock is 650 m^2 , this paddock would contribute a FCH_4 of $1.67 \text{ } \mu\text{mol m}^{-2} \text{ s}^{-1}$. This initial calculation suggests the cattle produce significantly greater FCH_4 compared to this urban wetland. Additional potential methane contributors from this sector include a sedimentation basin and trash rack which are a component of the Urrbrae Wetlands infrastructure; these contributions are impossible to separate from the total flux measured in this sector.

Urban regions offer a variety of potential methane sources, including gas leaks, car exhausts, and smaller domestic water sources like ponds. Flux estimates from the urban sector were collected infrequently as the wind only came from that area approximately 20% of the time. 127 samples had sufficient information to successfully estimate a footprint value. The urban fluxes recorded are similar to the wetland sector, which may be attributed to the location of the tower over the main pond, however the true origin of these fluxes can only be speculated. To the west of the tower there is 22 m of water before the lakes edge which most likely contributes to the total flux. The high fluxes recorded are likely a combination of some flux from this small section of pond, as well as some “urban” contribution, possibly from a potential pipeline leakage. However, to complicate matters, the area directly next to the tower contributes only small amounts to the total flux. Most measurement contributions come not from directly beneath the tower, nor from many kilometres away, but from an intermediary distance (Burba, 2013). This is because for the eddy to reach the sensor it must have both vertical and horizontal space to carry the gas up to the sensor. Due to these conflicting factors and limited information gathered, the contribution of urban fluxes to this system are not examined further.

6.3 DIURNAL PATTERNS

Previous studies, like that by Morin et al. (2014) have shown diurnal patterns exist in natural and reconstructed wetland systems. A strong diurnal peak is present in the early afternoon, between 14:00 and 15:00. The data is highly variable for this peak, being approximately two times larger than the rest of the day (Figure 5). The linear regression analysis (Figure 7b) supports the observation of a diurnal cycle primarily associated with air temperature (Figure 5). Due to the relatively tall vegetation found on the edges

of the wetland, and the sunrise time during winter at this latitude, full sunlight appears to warm the bottom of the wetland between 09:00 and 15:00 resulting in increased FCH₄ rates.

6.4 LONGER-TERM PATTERNS

It was difficult to discern any longer-term variability patterns in this data due to the paucity of the data as a result of the instrumental and power failures causing large data gaps. Attempts at filling the gaps in the time series were made by spline interpolation, however this proved to be an inappropriate technique to use, resulting in unrealistic curves (Examples can be seen in Appendix F). From the measured data, random higher emission days were observed. These are potentially due to the correlations observed with wind speed (Figure 7a) and air pressure (Figure 7c), however may also be due to weather patterns not measured in this study. To elucidate these factors, a longer study is needed to obtain a more continuous dataset. Under natural and reconstructed systems the peak flux values have been observed in the summer months, and lower flux values in the winter (Morin et al., 2014) so the same would be expected here.

6.2 THE IMPACT OF CLIMATIC FACTORS ON WETLAND METHANE FLUX

Many factors could be contributing to the significantly high flux rate measured in this study. These include vegetation species, OM input, air and sediment temperatures, wind speeds, temperature, and air pressure. Of these, temperature, wind speed and air pressure were specifically addressed in this study.

The relationship between FCH₄ and temperature observed in this study (Figure 7b) is consistent with a number of previous studies using various methodologies (Aben et al.,

2017; Morin et al., 2014; Yvon-Durocher et al., 2014). This relationship is important to understand due to the currently warming climate and extreme weather events. We observed a positive linear relationship in the measured data, between air temperature and FCH₄ (Figure 7b). This is the strongest correlation of all the factors recorded in this study. Nevertheless, the relationship is not strong, and there is significant variability in the relationship, most likely due to the narrow temperature range observed (5 to 20 °C). This narrow temperature range may have a greater significance than first thought as it has been shown that the presence of emergent vegetation moderates the heating and cooling of the water column (Burba, Verma, & Kim, 1999), which in turn would affect the sediment temperatures. Investigation of this key controlling factor is needed across a wider temperature range and study duration. The variability in the data suggests there may be other factors influencing the rate of methane flux in this environment.

In addition to the effects of temperature on methane production in wetland sediments, the release of methane from those sediments is influenced by wind stress and air pressure variability. The primary pathway of gas exchange in this system is ebullition, where bubbles form in the sediments, float to the surface, and burst, and are then integrated into the atmosphere. Wind is one of two near-surface stirring processes which drive these air-water gas transfers (Poindexter et al., 2013). According to Poindexter et al. (2013), in sites containing significant amounts of emergent vegetation (like Urrbrae), this mechanism is usually overwhelmed by the effect of thermal convection. However, as thermal convection was not measured as part of this experiment, no conclusion can be drawn on the relative importance of these controls. Examination of Figure 7b showed that wind speed and FCH₄ are positively, linearly correlated, hence as wind speed

increases, the FCH₄ also increases. Although the correlation is not strong ($r^2 = 0.265$), examination with the Pearson correlation coefficient determined the relationship was still statistically significant ($p \ll 0.05$).

Air pressure was also found to have a significant influence on FCH₄ (Figure 7c), despite the large scatter. This relationship demonstrates a small negative correlation between pressure and FCH₄ ($r^2 = -0.221$), however the use of the Pearson correlation coefficient ($p \ll 0.05$) indicates statistically significant correlation. These results are consistent with a study by Tokida et al. (2007) which show that decreases in atmospheric pressure leads to gas generation from solution in the form of episodic ebullitive fluxes. That is, significant upward migration of gas-phase methane and eventual rupture occur sequentially after drops in atmospheric pressure at the surface.

6.5 CARBON ISOTOPE RATIOS IN WETLAND METHANE

Gas isotope data was collected as part this study (Table 3). The isotope data provides a good indicator of the source of the methane produced. As expected, the results confirm that the primary source of the sedimentary methane is biogenic, with some mixing apparent in the air samples. The higher $\delta^{13}\text{C-CH}_4$ air sample isotope values is interpreted as sediment gas, which is predominantly biogenic carbon, mixed with multiple sources, including thermogenically sourced methane. Biological organisms are known to take up lighter carbon, ^{12}C , as part of photosynthesis. Wetlands are known to have $\delta^{13}\text{C}$ ratios of -50 to -80‰ dependent on methane production pathway (acetate fermentation or carbonate reduction)(Stevens & Engelkemeir, 1988; M. J. Whiticar, Faber, & Schoell, 1986; Michael J. Whiticar, 1999). The $\delta^{13}\text{C-CH}_4$ for samples

collected from the wetlands sediment are consistent with biogenic methane produced via acetate fermentation (Happell, Chanton, & Showers, 1994; M. J. Whiticar et al., 1986). Cattle produce $\delta^{13}\text{C}$ values of -45 to -76‰ depending on their diet (Stevens et al., 1988). The recorded atmospheric methane on-site is consistent with the present global atmospheric isotope ratio ~ -47 (Nisbet et al., 2016). Isotope exchange and mixing processes occur once methane is transferred into the atmosphere and the molecules are able to react with hydroxyl radicals present to form water vapour and carbon dioxide, however this is not the focus of this study (Blackwell, 2011).

6.6 IMPLICATIONS

Artificial urban wetlands are being constructed at increasing rates to restore systems which have been lost due to anthropogenic activities. These spaces provide habitat for a variety of flora and fauna, potentially act as carbon burial sites, and provide 'green spaces' in a growing urban environment. However, the data collected in this study implies that while these spaces are visually and ecologically beneficial, they can be significant sources of atmospheric methane. Current climate data indicates that global temperatures have increased by $0.6\text{ }^{\circ}\text{C}$ since pre-industrial levels and will continue to rise over coming years (IPCC, 2014b). The positive relationship between temperature and methane flux indicates that methane production in these systems should be of significant concern when constructing current and future carbon budgets for urban settings, especially local carbon budgets. The magnitude and number of artificial wetlands in an area will also affect the scale of impact. FCH_4 rates could be partially mitigated by infrastructure to aerate the sediments and control nutrient loading to reduce the anaerobic methanogenic processes, however more research is required into the

environmental controls before an effective mitigation strategy is developed (Wassmann, Papen, & Rennenberg, 1993).

6.7 FUTURE RESEARCH

There are many different avenues that this type of research can extend into in the future.

To address issues experienced and questions which have surfaced in this study, longer-term monitoring of the site is required, with the addition of a slow auxiliary biometric system (Biomet), which records sediment and water temperatures (Burba, 2005).

Biomet systems also aid in data recovery and provide information for more advanced gap filling techniques (G. Burba, 2005). These equipment additions, supported by a hard-line power source to the EC tower, would eliminate the issues of power failure, and provide a more continuous dataset. An extended study could also provide a better understanding of these sites under a wider range of meteorological conditions.

Observing the behaviour of the site over the extreme temperatures in the summer months could provide a better prediction about the behaviour of these sites in a warming climate. Replicating and extending these methods to examine other artificial urban wetlands is also needed to draw broader conclusions about the behaviours of these ecosystems. A biological route could also be explored, investigating and identifying the species of methanogenic bacteria present in the Urrbrae Wetland (or other artificial wetland), and investigate how the content and rates of carbon input and type of input affect the methane production rates. Understanding these processes could provide evidence for decision-makers and planners to enforce strategies to reduce the methane output while maximising the potential for the site to act as a carbon burial hub.

7 CONCLUSIONS

Methane fluxes in the artificially constructed Urrbrae Wetlands were measured nearly continually over three months using the open-path Eddy Covariance method. Mean FCH_4 of the wetland was found to be $0.2603 \pm 0.1865 \mu\text{mol m}^{-2} \text{s}^{-1}$ which is a factor of 10 higher than previously reported values for natural and restored wetland ecosystems. While a small difference between mean night and daytime FCH_4 was measured, the difference was not substantial enough to exhibit statistical significance, further supporting previous observations (Morin et al., 2014; Yvon-Durocher et al., 2014) that night fluxes significantly contribute to overall flux. Linear correlations between FCH_4 and air temperature, air pressure and wind speed suggest that each of these factors contribute to the measured FCH_4 . Early afternoon peaks occurred diurnally with the mean maximum daily temperature, further supporting existing published materials addressing the association between temperature and flux (Yvon-Durocher et al., 2014), highlighting the importance of mitigating flux output in a warming climate. As our record was not continuous enough, we were unable to make conclusions regarding longer term flux variations. In future it will be helpful to evaluate these patterns to build a complete picture of the processes occurring in these types of artificial environments. We conclude that artificial urban wetlands are potentially a significant source of atmospheric methane which requires further investigation. Preliminary results indicate that strategies to mitigate methane release require investigation and implementation in these systems to minimise or neutralise the output of methane for the optimisation of these system as a carbon sink.

8 ACKNOWLEDGMENTS

I would like to thank the following people and companies for their assistance in making this project possible.

- To Michael Hatch and Jonathan Tyler, my supervisor and co-supervisor respectively, thank you both for your constant support, patience, guidance, expertise and time throughout the project.
- Karita Parker for your contributions and guidance in this endeavour.
- Martin Kennedy from Macquarie University for loaning us the flux towers which have made this project possible.
- Staff at the University of Adelaide's Department of Earth Sciences and Department of Physics, (both School of Physical Sciences). Particularly Murray Hamilton, Derrick Hasterok, and Sujata Kovalam for your guidance and assistance throughout the year.
- The Urrbrae Agricultural School and Mitcham City Council for letting us conduct tests on their property, with special thanks to Vanessa Greenslade for being so accommodating with your time and knowledge of the study site.

9 REFERENCES

- ABEN, R. C. H., BARROS, N., VAN DONK, E., FRENKEN, T., HILT, S., KAZANJIAN, G., ... KOSTEN, S. (2017). Cross continental increase in methane ebullition under climate change. *Nature Communications*, 8(1), 1–8. <https://doi.org/10.1038/s41467-017-01535-y>
- ALBERTO, M. C. R., WASSMANN, R., BURESH, R. J., QUILTY, J. R., CORREA, T. Q., SANDRO, J. M., & CENTENO, C. A. R. (2014). Measuring methane flux from irrigated rice fields by eddy covariance method using open-path gas analyzer. *Field Crops Research*, 160, 12–21. <https://doi.org/10.1016/j.fcr.2014.02.008>
- AUBINET, M., VESALA, T., & PAPALE, D. (2012). *Eddy Covariance: A Practical Guide to Measurement and Data Analysis* (2012th ed.; M. Aubinet, T. Vesala, & D. Papale, Eds.). <https://doi.org/10.1007/978-94-007-2351-1>
- BALDOCCHI, D. D. (2003). Assessing the eddy covariance technique for evaluating carbon dioxide exchange rates of ecosystems: Past, present and future. *Global Change Biology*, 9(4), 479–492. <https://doi.org/10.1046/j.1365-2486.2003.00629.x>
- BLACKWELL, M. S. A. (2011). Wetland Ecosystems. In *Journal of Environment Quality* (Vol. 40, p. 1028). <https://doi.org/10.2134/jeq2011.0002br>
- BURBA, G. (2005). *Eddy Covariance Method - for Scientific, Industrial, Agricultural, and Regulatory Applications*. Lincoln, Nebraska: LI-COR Biosciences.
- BURBA, G. (2013). *Eddy Covariance Method - Step-by-Step Field book to Flux Measurements* (L.-C. Biosciences, Ed.). Retrieved from http://www.licor.com/env/products/eddy_covariance/ec_book.html?form=2
- BURBA, G. G., VERMA, S. B., & KIM, J. (1999). A comparative study of surface energy fluxes of three communities (*Phragmites australis*, *Scirpus acutus*, and open water) in a prairie wetland ecosystem. *Wetlands*, 19(2), 451–457. <https://doi.org/10.1007/BF03161776>
- BUREAU OF METEOROLOGY. (2019). Climate Data Online. Retrieved August 29, 2019, from <http://www.bom.gov.au/climate/data/>
- CLARK, B. (2014). *Using Cavity Ring Down Spectroscopy to measure greenhouse gas concentrations and estimate flux to the atmosphere using a closed flux chamber*. The University of Adelaide.
- DEEMER, B. R., HARRISON, J. A., LI, S., BEAULIEU, J. J., DELSONTRO, T., BARROS, N., ... VONK, J. A. (2016). Greenhouse gas emissions from reservoir water surfaces: A new global synthesis. *BioScience*, 66(11), 949–964. <https://doi.org/10.1093/biosci/biw117>
- DILLON, P., PAVELIC, P., MASSMANN, G., BARRY, K., & CORRELL, R. (2001). Enhancement of the Membrane Filtration Index Method. *Desalination*, 140, 153–165.
- FEITZ, A., SCHRODER, I., PHILLIPS, F., COATES, T., NEGHANDHI, K., DAY, S., ... GRIFFITH, D. (2018). The

- Ginninderra CH₄ and CO₂ release experiment: An evaluation of gas detection and quantification techniques. *International Journal of Greenhouse Gas Control*, 70(August 2017), 202–224. <https://doi.org/10.1016/j.ijggc.2017.11.018>
- GE, H. X., ZHANG, H. S., ZHANG, H., CAI, X. H., SONG, Y., & KANG, L. (2018). The characteristics of methane flux from an irrigated rice farm in East China measured using the eddy covariance method. *Agricultural and Forest Meteorology*, 249(April 2017), 228–238. <https://doi.org/10.1016/j.agrformet.2017.11.010>
- HAPPELL, J. D., CHANTON, J. P., & SHOWERS, W. S. (1994). The influence of methane oxidation on the stable isotopic composition of methane emitted from Florida swamp forests. *Geochimica et Cosmochimica Acta*. [https://doi.org/10.1016/0016-7037\(94\)90341-7](https://doi.org/10.1016/0016-7037(94)90341-7)
- HATCH, M. A., KENNEDY, M. J., HAMILTON, M. W., & VINCENT, R. A. (2018). Methane variability associated with natural and anthropogenic sources in an Australian context. *Australian Journal of Earth Sciences*, 65(5), 683–690. <https://doi.org/10.1080/08120099.2018.1471004>
- HERBST, M., FRIBORG, T., RINGGAARD, R., & SOEGAARD, H. (2011). Interpreting the variations in atmospheric methane fluxes observed above a restored wetland. *Agricultural and Forest Meteorology*, 151(7), 841–853. <https://doi.org/10.1016/j.agrformet.2011.02.002>
- HOLGERSON, M. A., & RAYMOND, P. A. (2016). Large contribution to inland water CO₂ and CH₄ emissions from very small ponds. *Nature Geoscience*, 9(3), 222–226. <https://doi.org/10.1038/ngeo2654>
- IPCC. (2014a). Climate Change 2014: Synthesis Report; Chapter Observed Changes and their Causes. In *Ipcc*. <https://doi.org/10.1046/j.1365-2559.2002.1340a.x>
- IPCC. (2014b). Climate Change 2014 Part A: Global and Sectoral Aspects. In *Climate Change 2014: Impacts, Adaptation, and Vulnerability. Part A: Global and Sectoral Aspects. Contribution of Working Group II to the Fifth Assessment Report of the Intergovernmental Panel on Climate Change*. <https://doi.org/10.1007/s13398-014-0173-7.2>
- ISAKSEN, I. S. A., BERNTSEN, T. K., DALSSØREN, S. B., ELEFATHERATOS, K., ORSOLINI, Y., ROGNERUD, B., ... HOLMES, C. D. (2014). Atmospheric ozone and methane in a changing climate. *Atmosphere*, 5(3), 518–535. <https://doi.org/10.3390/atmos5030518>
- KIRSCHKE, S., BOUSQUET, P., CIAIS, P., SAUNOIS, M., CANADELL, J., DLUGOKENCKY, E., ... ZENG, J. (2013). Three decades of global methane sources and sinks. *Nature Geoscience*, 6(10), 813–823. <https://doi.org/10.1038/ngeo1955>
- KLJUN, N., CALANCA, P., ROTACH, M. W., & SCHMID, H. P. (2004). A simple parameterisation for flux footprint predictions. *Boundary-Layer Meteorology*, 112(3), 503–523. <https://doi.org/10.1023/B:BOUN.0000030653.71031.96>
- LICOR. (2019). *EddyPro Software*. Lincoln, Nebraska.
- LOHILA, A., LAURILA, T., TUOVINEN, J. P., AURELA, M., HATAKKA, J., THUM, T., ... VESALA, T. (2007). Micrometeorological measurements of methane and carbon dioxide fluxes at a municipal landfill. *Environmental Science and Technology*, 41(8), 2717–2722. <https://doi.org/10.1021/es061631h>
- MASSMAN, W. J. (2000). A simple method for estimating frequency response corrections for eddy covariance systems. *Agricultural and Forest Meteorology*, 104(3), 185–198. [https://doi.org/10.1016/S0168-1923\(00\)00164-7](https://doi.org/10.1016/S0168-1923(00)00164-7)
- MCGINN, S. M., BEAUCHEMIN, K. A., COATES, T., & MCGEOUGH, E. J. (2014). Cattle methane emission and pasture carbon dioxide balance of a grazed grassland. *Journal of Environmental Quality*, 43(3), 820–828. <https://doi.org/10.2134/jeq2013.09.0371>
- MELTON, J. R., WANIA, R., HODSON, E. L., POULTER, B., RINGEVAL, B., SPAHNI, R., ... KAPLAN, J. O. (2013). Present state of global wetland extent and wetland methane modelling: Conclusions from a model inter-comparison project (WETCHIMP). *Biogeosciences*, 10(2), 753–788. <https://doi.org/10.5194/bg-10-753-2013>
- MITCHAM CITY COUNCIL. (2019). City of Mitcham: Urrbrae Wetland Facts. Retrieved April 10, 2019, from <https://www.mitchamcouncil.sa.gov.au/urrbraewetlandfacts>
- MITSCH, W. J., BERNAL, B., NAHLIK, A. M., MANDER, Ü., ZHANG, L., ANDERSON, C. J., ... BRIX, H. (2013). Wetlands, carbon, and climate change. *Landscape Ecology*, 28(4), 583–597. <https://doi.org/10.1007/s10980-012-9758-8>
- MONCRIEFF, J., VALENTINI, R., GRECO, S., GUENTHER, S., & CICCIOLO, P. (1997). Trace gas exchange over terrestrial ecosystems: methods and perspectives in micrometeorology. *Journal of Experimental Botany*, 48(5), 1133–1142. <https://doi.org/10.1093/jxb/48.5.1133>
- MORIN, T. H., BOHRER, G., NAOR-AZRIELI, L., MESI, S., KENNY, W. T., MITSCH, W. J., & SCHÄFER, K. V. R. (2014). The seasonal and diurnal dynamics of methane flux at a created urban wetland.

- Ecological Engineering*, 72, 74–83. <https://doi.org/10.1016/j.ecoleng.2014.02.002>
- MORIN, T. H., BOHRER, G., STEFANIK, K. C., REY-SANCHEZ, A. C., MATHENY, A. M., & MITSCH, W. J. (2017). Combining eddy-covariance and chamber measurements to determine the methane budget from a small, heterogeneous urban floodplain wetland park. *Agricultural and Forest Meteorology*, 237–238, 160–170. <https://doi.org/10.1016/j.agrformet.2017.01.022>
- NEGANDHI, K., EDWARDS, G., KELLEWAY, J. J., HOWARD, D., SAFARI, D., & SAINTILAN, N. (2019). Blue carbon potential of coastal wetland restoration varies with inundation and rainfall. *Scientific Reports*, 9(1), 1–9. <https://doi.org/10.1038/s41598-019-40763-8>
- NISBET, E. G., DLUGOKENCKY, E. J., MANNING, M. R., LOWRY, D., FISHER, R. E., FRANCE, J. L., ... GANESAN, A. L. (2016). Rising atmospheric methane: 2007–2014 growth and isotopic shift. *Global Biogeochemical Cycles*, 30(9), 1356–1370. <https://doi.org/10.1002/2016GB005406>
- PAWLAK, W., FORTUNIAK, K., SIEDLECKI, M., & ZIELIŃSKI, M. (2016). Urban – Wetland contrast in turbulent exchange of methane. *Atmospheric Environment*, 145(September 2015), 176–191. <https://doi.org/10.1016/j.atmosenv.2016.09.036>
- POINDEXTER, C. M., & VARIANO, E. A. (2013). Gas exchange in wetlands with emergent vegetation: The effects of wind and thermal convection at the air-water interface. *Journal of Geophysical Research: Biogeosciences*, 118(3), 1297–1306. <https://doi.org/10.1002/jgrg.20099>
- SHAO, X., SHENG, X., WU, M., WU, H., & NING, X. (2017). Methane production potential and emission at different water levels in the restored reed wetland of Hangzhou Bay. *PLoS ONE*, 12(10), 1–13. <https://doi.org/10.1371/journal.pone.0185709>
- SILVEY, C., JARECKE, K. M., HOPFENSBERGER, K., LOECKE, T. D., & BURGIN, A. J. (2019). Plant species and hydrology as controls on constructed wetland methane fluxes. *Soil Science Society of America Journal*, 83(3), 848–855. <https://doi.org/10.2136/sssaj2018.11.0421>
- STEVENS, C. M., & ENGELKEMEIR, A. (1988). Stable carbon isotopic composition of methane from some natural and anthropogenic sources. *Journal of Geophysical Research*, 93(D1), 725. <https://doi.org/10.1029/jd093id01p00725>
- TANG, A. C. I., STOY, P. C., HIRATA, R., MUSIN, K. K., AERIES, E. B., WENCESLAUS, J., & MELLING, L. (2018). Eddy Covariance Measurements of Methane Flux at a Tropical Peat Forest in Sarawak, Malaysian Borneo. *Geophysical Research Letters*, 45(9), 4390–4399. <https://doi.org/10.1029/2017GL076457>
- THE EUROPEAN WIND ENERGY ASSOCIATION. (n.d.). Wind Energy. Retrieved August 1, 2019, from <https://www.wind-energy-the-facts.org/fundamentals.html>
- TOKIDA, T., MIYAZAKI, T., MIZOGUCHI, M., NAGATA, O., TAKAKAI, F., KAGEMOTO, A., & HATANNO, R. (2007). Falling atmospheric pressure as a trigger for methane ebullition from peatland. *Global Biogeochemical Cycles*, 21(2), 1–8. <https://doi.org/10.1029/2006GB002790>
- WASSMANN, R., PAPAN, H., & RENNENBERG, H. (1993). Methane emission from rice paddies and possible mitigation strategies. *Chemosphere*, 26(1–4), 201–217. [https://doi.org/10.1016/0045-6535\(93\)90422-2](https://doi.org/10.1016/0045-6535(93)90422-2)
- WEBB, E., PEARMAN, G., & LEUNING, R. (1980). Correction of flux measurements for density effects due to heat and water vapour transfer. *Quarterly Journal of the Royal Meteorological Society*, 106, 85–100. <https://doi.org/551.510.3 : 551.511.61>
- WHITICAR, M. J., FABER, E., & SCHOELL, M. (1986). Biogenic methane formation in marine and freshwater environments: CO₂ reduction vs. acetate fermentation-Isotope evidence. *Geochimica et Cosmochimica Acta*. [https://doi.org/10.1016/0016-7037\(86\)90346-7](https://doi.org/10.1016/0016-7037(86)90346-7)
- WHITICAR, MICHAEL J. (1999). Carbon and hydrogen isotope systematics of bacterial formation and oxidation of methane. *Chemical Geology*, 161(1), 291–314. [https://doi.org/10.1016/S0009-2541\(99\)00092-3](https://doi.org/10.1016/S0009-2541(99)00092-3)
- WHITING, B. G. J., & CHANTON, J. P. (2001). *Greenhouse carbon balance of wetlands: methane emission versus carbon sequestration - WHITING - 2003 - Tellus B - Wiley Online Library*. 521–528.
- XU, L., LIN, X., AMEN, J., WELDING, K., & MCDERMOTT, D. (2014). Impact of changes in barometric pressure on landfill methane emission Liukang. *Global Biogeochemical Cycles*, (28), 679–695. <https://doi.org/10.1002/2013GB004571>
- YAO, H., & CONRAD, R. (2000). Effect of temperature on reduction of iron and production of carbon dioxide and methane in anoxic wetland rice soils. *Biology and Fertility of Soils*, 32(2), 135–141. <https://doi.org/10.1007/s003740000227>
- YVON-DUROCHER, G., ALLEN, A. P., BASTVIKEN, D., CONRAD, R., GUDASZ, C., ST-PIERRE, A., ... DEL GIORGIO, P. A. (2014). Methane fluxes show consistent temperature dependence across microbial to ecosystem scales. *Nature*, 507(7493), 488–491. <https://doi.org/10.1038/nature13164>

ZHU, G., ZHANG, Z., ZIMMERMANN, N. E., STENKE, A., HODSON, E. L., LI, X., ... POULTER, B. (2017).
Emerging role of wetland methane emissions in driving 21st century climate change. *Proceedings
of the National Academy of Sciences*, 114(36), 9647–9652.
<https://doi.org/10.1073/pnas.1618765114>

APPENDIX A: SUPPLEMENTARY METHODS

Link to Raw and sorted data files.

The following link directs the reader to the main folder on Box containing the raw ghg files, the output by eddy pro in the form of excel csv files and the various sorted and filtered excel files used to manage data and perform statistical analysis.

<https://universityofadelaide.box.com/s/h2zovv00yz5fos044mmmm7thidr18099>

Sensitivity Study on roughness length

In the EddyPro program there are three estimated parameters that quantify various aspects of a field site. These include canopy height, displacement height and roughness length. The most important of these estimates is the “roughness length” of the field area (Z_0). This is a parameter that is defined as the height at which a specifically described surface wind goes to zero and is strongly dependent on the “roughness” of features inside the area sampled by the various eddies that pass through (G. Burba, 2005). As the Urrbrae site is relatively heterogeneous containing flat water, shrubs, reeds, and tall trees, it was difficult to estimate a single value for the site that captured all of this variation. Due to the difficulty in determining this value a sensitivity study was performed on Z_0 that tested a range of values to see how they affected flux calculations for the data collected.

One estimate for roughness length is given by:

$$Z_0 = 0.15 \times \text{canopy height} \quad (7)$$

To estimate the canopy height associated with a given roughness, equation 7 was inverted to give canopy height. Some number of given various Z_0 values were tested, ranging from 0.005 to 0.8 (The European Wind Energy Association, n.d.). A sample of 1 month of data (July 2019) was processed using the methods outlined in sections 4.1 and 4.2 using different intervals of Z_0 and associated canopy height. The effects of altering these factors can be seen in Table 5.

Table 5: Mean FCH₄ and error in the mean associated with varying roughness length.

Z_0 (m)	Canopy Height (m)	Displacement Height (m)	Average Methane Flux ($\mu\text{mol.m}^{-2}.\text{s}^{-1}$)	Standard Deviation ($\mu\text{mol.m}^{-2}.\text{s}^{-1}$)	Used for
0.8	5.33	3.57	0.370365	0.229842	Suburb
0.5	3.33	2.23	0.362417	0.226792	Forested Woodland
0.1	0.66	0.45	0.26235	0.16665	Farmland
0.06	0.4	0.27	0.25926	0.164556	Australian Average
0.05	0.33	0.22	0.258473	0.164024	Open farmland
0.005*	0.03	0.02	0.255592	0.16208	Still water

*not possible to input due to only 2 decimal places in Eddy pro interface. Recorded as 0.00m.

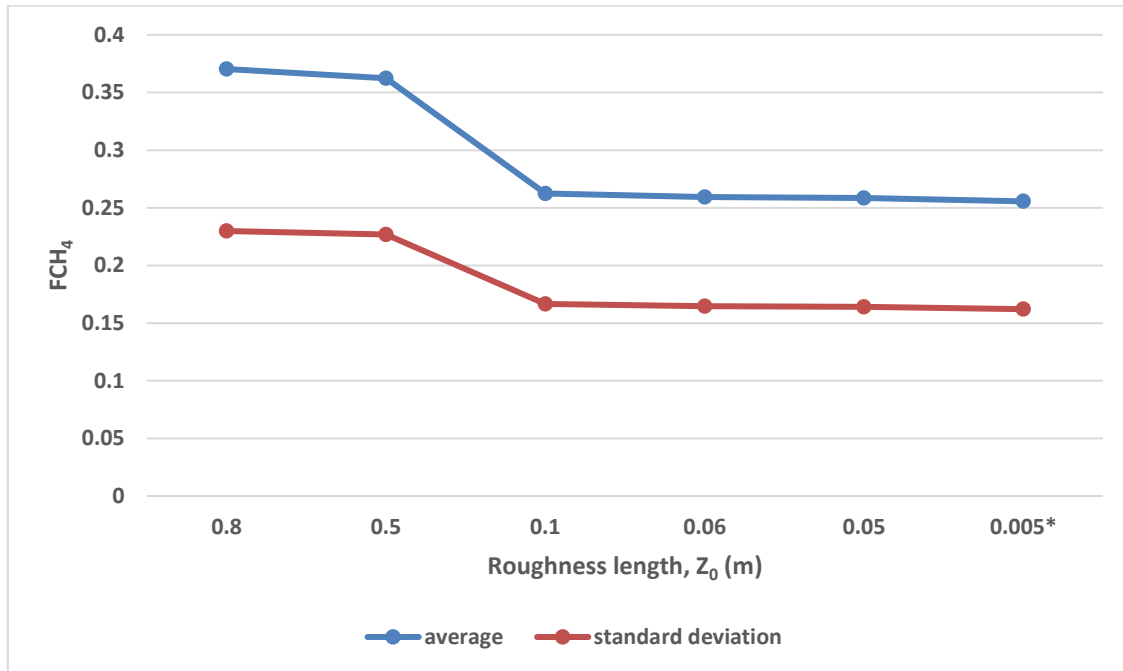


Figure 8: The relationship between decreasing roughness length with methane flux indicates a threshold value where the F_{CH_4} decrease outside the levels of instrument sensitivity.

A range of values were tested and it was found that it did not affect the final flux values greatly. Roughness length of 0.05 was selected for EddyPro processing as the flux did not decrease to expected amounts, however did appear to plateau around 0.05 and 0.005 outside the levels of instrument sensitivity (Sensitivity study results found in Appendix A).

Discussion of sensitivity results:

The flux that we have measured for Urrbrae Wetlands is significantly higher than for other wetlands. The sensitivity study outlined was an additional means to explore and confirm our findings of significantly greater flux. By altering the roughness length by a factor of 10 and 100, we were able to examine the impact it has on our data set. This impact was discovered to be minimal on the scales we are working with and as such supported the estimated flux values.

APPENDIX B: SITE DISTRIBUTION AND INFRASTRUCTURE

Figure 9 contains an image of the Urrbrae Wetlands study site with the full infrastructure indicated.

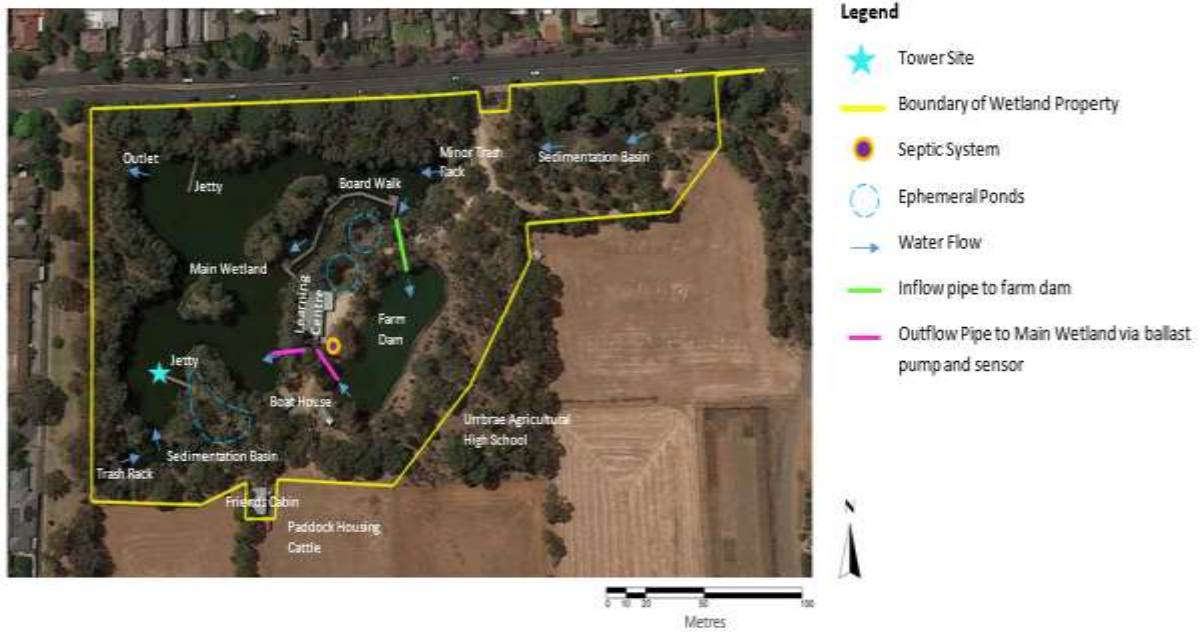


Figure 9: Full infrastructure map of the Urrbrae Wetlands.

APPENDIX C: ALTERNATE METHODOLOGY FOR SEDIMENT AND AIR GAS COLLECTION AND ANALYSIS

Urrbrae Air Samples:

Box method air samples are collected using an instrument designed by Dr Murray Hamilton from the University of Adelaide (Figure 10). This method involves using gas collection bags which are inside a plastic box and attached to a valve. Using a bike pump, the air is removed from the box creating a vacuum, forcing the outside air to be pulled into the gas collection bag from the outside system. In our experiment, one person held the box close to the Li7700 methane analyser, while another operated the bike pump. This allowed the samples collected to be from the same vicinity as those collected by the Li7700.

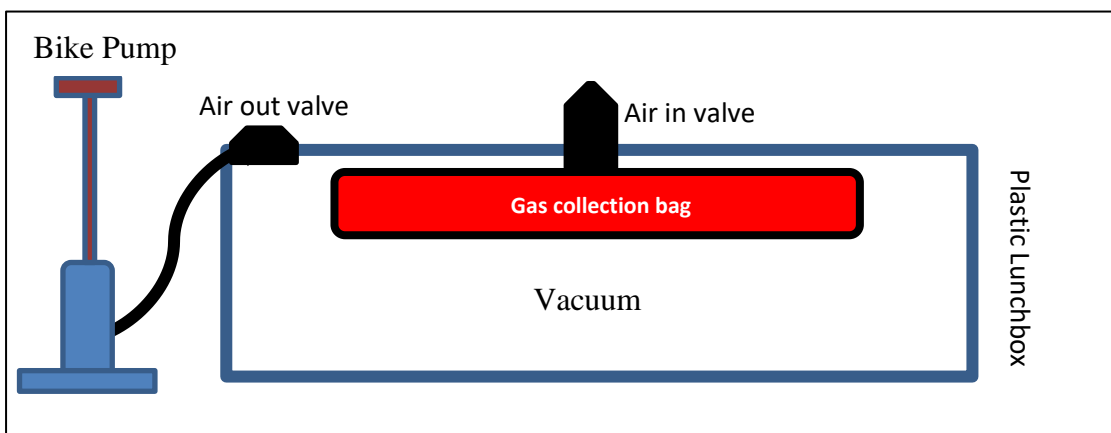


Figure 10: Schematic of the gas collection instrument designed by Dr Murray Hamilton used to collect air samples from near the Li7700 methane analyser.

Urrbrae sediment gas sampling:

The bottle air samples were collected using a rudimentary column displacement method. A funnel (diameter 30 cm) is attached to a standard commercial clean, empty plastic water bottle (250 mL), with a handle supporting for ease of use. The equipment was inverted underwater and allowed to fill. Using my feet, the sediment was disturbed under the area of the funnel to encourage the bubbles to rise into the bottle and displace the water. Once filled with gas, the bottle is unscrewed from the funnel and capped while still underwater, hence no gas was lost or contaminated.

The area sampled for each bottle was approximately 2 x 4 m. These samples were then tested using the Picarro cavity ring down spectrometer.

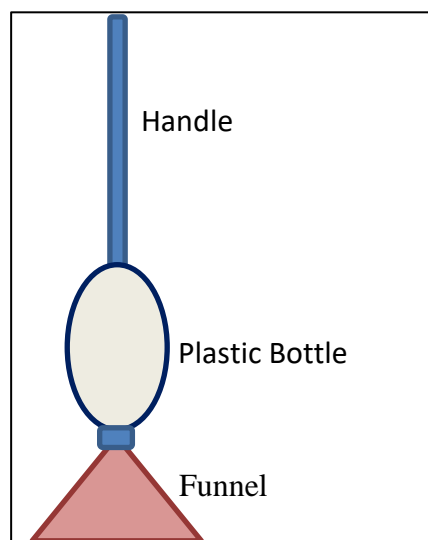


Figure 11: Schematic of the instrument used for the volume displacement method.

Picarro cavity ring down spectrometer:

The Picarro was first allowed to sample the room air, and then flushed with the small BOC standard tank reading 2.075 ppm CH₄. The air samples were able to be analysed by drawing air directly from the gas sample bags into the CRDS. The bottle sediment gas sampled had to be diluted. Using a gas sampling needle, 500mL of zero air was inserted into a fresh gas bag, along with 0.2 mL of the bottled sample. The bottled sample was removed by piercing the bottle plastic with the syringe, withdrawing the sample than covering the hole with electrical tape.

Picarro Theory:

The Picarro is a cavity ring down spectrometry (CRDS) based GHG analyser. Basically, it measured the time taken for a NIR laser signal to decay in a gas filled optical cavity after the laser is terminated (Picarro inc, 2014). The strength of adsorption at the NIR spectrum is used to determine concentration by application of the following fundamental theorem:

$$I(t, \lambda) = I_0 e^{-t/\tau(\lambda)} \quad (8)$$

$I(t, \lambda)$ is the light intensity in the cavity after time t , I_0 is the light transmitted when the laser is terminated, and $\tau(\lambda)$ is the ring-down constant.

A number of frequencies were used to measure for corresponding NIR peaks for the C¹² and C¹⁴ in CO₂ and CH₄ each for calculation of total gas concentration and isotopic signature identification.

The isotopic signatures are useful to determine if the origins are biogenic or thermogenic. The range however is limited for the Picarro for 1.8 – 12.0 ppm in HP mode and 10-1000 in HR.

Results are presented onscreen in real time and recorded for later reference.

APPENDIX D: EXAMINATION OF OUTLIER VALUES

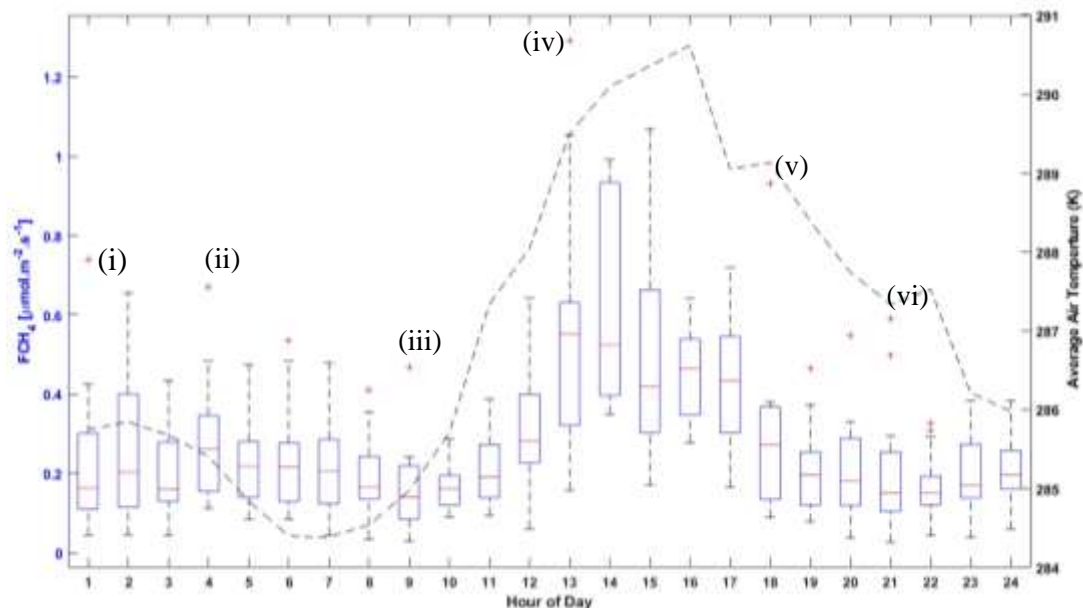


Figure 12: Figure 5 (Hourly diurnal fluxes plotted with hourly average temperature) with outlier reference codes.

Table 6: Sample of Figure 5 outliers and selected data on each interval.

Code	Hour	FCH ₄	Air Temp	Air Pressure	Wind Speed	u*	RSSI	wind direction
i	1	0.739517	285.347	100606	0.350265	0.205641	43.1881	81.1301
ii	4	0.669142	286.101	100413	0.662646	0.289281	43.3922	27.1615
iii	9	0.468463	282.123	101086	0.132598	0.097134	46.0137	350.829
iv	13	0.620629	288.86	100922	0.924834	0.311609	54.6775	352.492
v	18	0.932681	291.342	100448	0.548753	0.185412	54.0965	37.5916
vi	21	0.498217	289.079	100001	0.257439	0.047286	40.5103	67.344

Observations:

Temperatures for these outliers range from 12 – 18 °C. All occur at similar pressure. All other factors variate significantly and so are unlikely to be the dominating factor. Temperatures around these values do not change significantly, but examination of the raw data shows a slight pressure decrease in the 30 minute interval before or during the spike. The time of day that these images occur are varying.

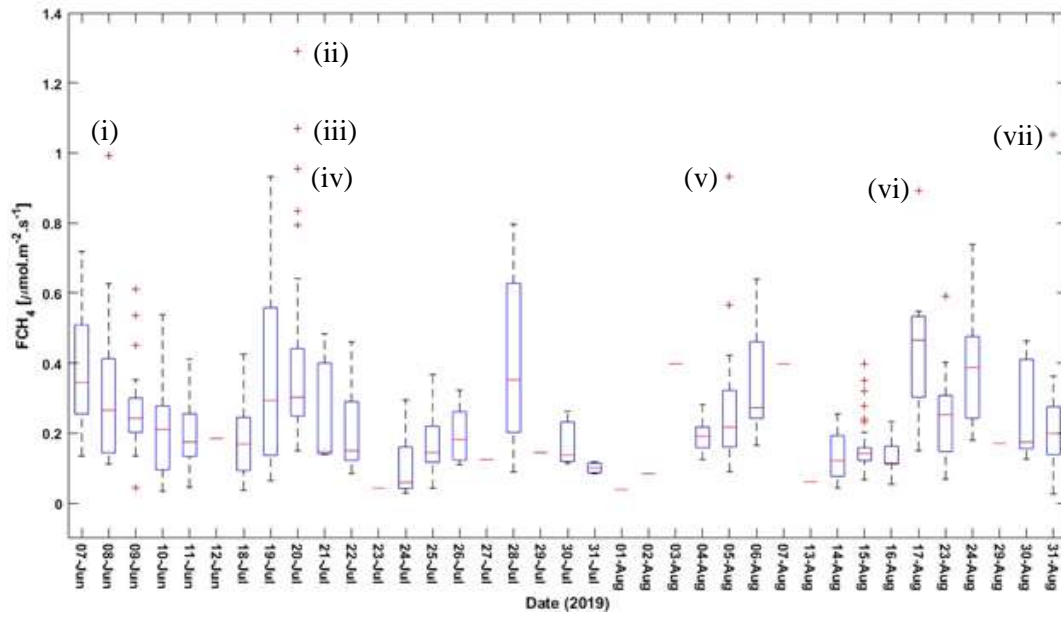


Figure 13: Copy of figure 6 (Daily flux distribution) with outlier codes.

Table 7: Sample of Figure 6 outliers with selected conditional data for each interval.

Outlier Code	Date	FCH4	Air Temp Record	Air Pressure	Wind Speed	Direction	Time Recorded	u*	RSSI	Day Ave Temp
i	8-Jun	0.9932	288.558	101292	0.732258	356.513	13:30	0.251826	58.6842	286
ii	20-Jul	1.29211	290.947	99945.3	1.56056	358.743	13:00	0.434745	55.4361	288
iii	20-Jul	0.954961	291.201	99876.1	1.93873	0.995567	13:30	0.510351	55.3989	288
iv	20-Jul	1.06963	291.622	99724.5	2.23721	357.572	14:30	0.466873	55.2863	288
v	5-Aug	0.933384	290.996	101093	0.776782	358.363	13:30	0.327667	47.8002	288
vi	17-Aug	0.890941	290.478	100215	0.985464	0.638199	15:00	0.340795	40.2978	283
vii	31-Aug	1.05233	292.388	100716	1.43172	350.969	12:30	0.424417	42.6362	289

Observations:

All the outliers occur with temperatures near 290 K (17 °C), around 10 kPa in pressure and all originate from the northerly winds. Additionally, they all occur in early to mid-afternoon (12:30 – 15:00) which is where the daily maximum temperatures occur. There is greater variability in the air pressure for these values. All sourced from early to mid-afternoon. All sourced from days where the average daily temperature is around 15 °C. Highest flux peaks of the above samples all come from periods of the lowest pressure. Examination of the raw data from surrounding intervals showed nothing immediately significant.

APPENDIX E: TWO SAMPLE T-TESTS ASSUMING UNEQUAL VARIANCE

Comparison of Day and Night data for statistical difference:

Table 8: Comparison of Day/Night data for each data set using Two-sample t-test assuming unequal variances. This was performed for all data combined, the wetland sector, the cattle sector and the urban sector.

Wetland Sector		
t-Test: Two-Sample Assuming Unequal Variances	Night	Day
Mean	0.219651	0.308116
Variance	0.019339	0.048892
Observations	228	194
Hypothesized Mean Difference	0	
df	314	
t Stat	-4.82016	
P(T<=t) one-tail	1.12E-06	
t Critical one-tail	1.649721	
P(T<=t) two-tail	2.24E-06	
t Critical two-tail	1.967548	
Cattle Sector		
t-Test: Two-Sample Assuming Unequal Variances	Night	Day
Mean	0.277318	0.169865
Variance	0.057501	0.019581
Observations	300	106
Hypothesized Mean Difference	0	
df	316	
t Stat	5.538527	
P(T<=t) one-tail	3.21E-08	
t Critical one-tail	1.64969	
P(T<=t) two-tail	6.43E-08	
t Critical two-tail	1.9675	
Urban Sector		
t-Test: Two-Sample Assuming Unequal Variances	Night	Day
Mean	0.257326369	0.2102734
Variance	0.05651679	0.03556926
Observations	280	256
Hypothesized Mean Difference	0	
df	524	
t Stat	2.548853312	
P(T<=t) one-tail	0.005545875	
t Critical one-tail	1.647766763	
P(T<=t) two-tail	0.011091751	
t Critical two-tail	1.964501517	

All Directions

t-Test: Two-Sample Assuming Unequal Variances	Night	Day
Mean	0.243245	0.251602

Variance	0.039768	0.042934
Observations	584	459
Hypothesized Mean Difference	0	
df	966	
t Stat	-0.65733	
P(T<=t) one-tail	0.255563	
t Critical one-tail	1.646433	
P(T<=t) two-tail	0.511126	
t Critical two-tail	1.962423	

Comparison of morning and evening wetland data for statistical difference:

Table 9: Comparison of Morning/Afternoon data for the wetland dataset using Two-sample t-test assuming unequal variances.

t-Test: Two-Sample Assuming Unequal Variances

<i>Wetland Sector</i>	<i>06:00 - 12:00</i>	<i>12:00 - 16:30</i>
Mean	0.308116392	0.513365406
Variance	0.048891867	0.05897189
Observations	194	64
Hypothesized Mean Difference	0	
df	100	
t Stat	-5.991667789	
P(T<=t) one-tail	1.64719E-08	
t Critical one-tail	1.660234326	
P(T<=t) two-tail	3.29439E-08	
t Critical two-tail	1.983971519	

APPENDIX F: SAMPLE OF ATTEMPTED GAP-FILLING TECHNIQUES

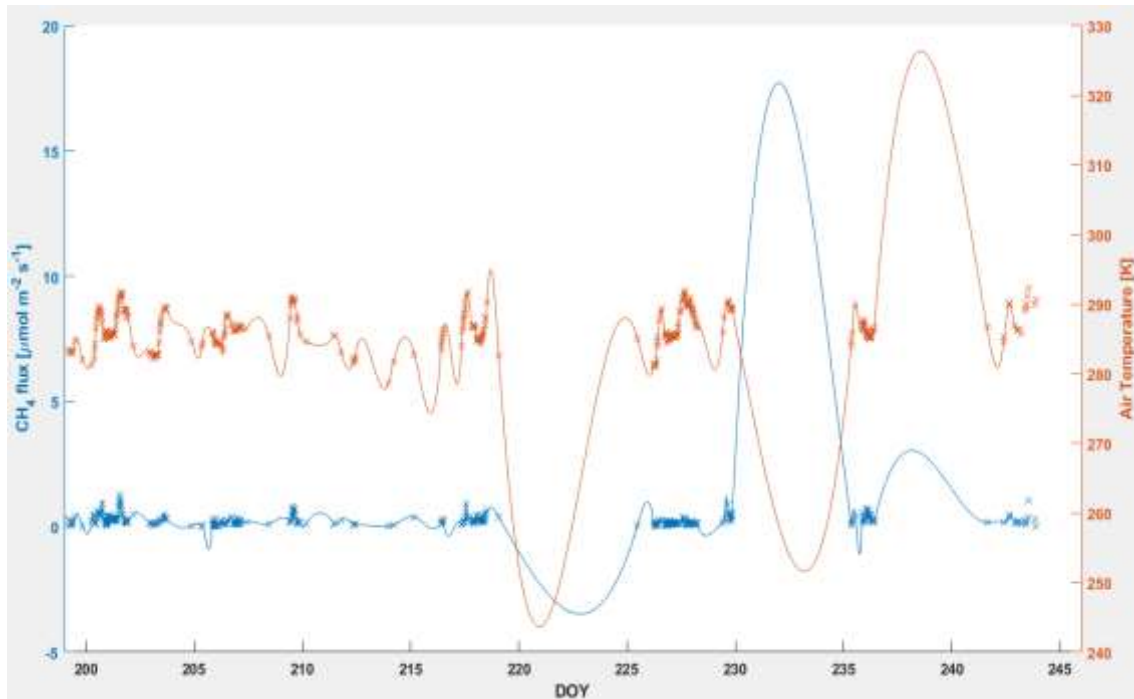


Figure 14: Comparison of air temperature with methane flux using spline. Crosses represent the original data sets.

In an attempt to gap-fill data for further analysis, various datasets were splined. This proved to be an inappropriate technique to use, resulting in unrealistic curves (Figure 14). Significant data gaps can be observed from DOY 220- 225, 231-235 and 237 – 242 which are major contributors to the inability to gap-fill (Figure 14). Other studies have used methods like employing artificial neural networks, estimation through other recorded data, or bootstrap or Monte Carlo techniques to gap-fill however these were not able to be attempted due to the magnitude of the gaps in our data (Kljun et al., 2004; Morin et al., 2017; Tang et al., 2018).